Point-Evolution Kernel Density Estimation based Time-Dependent Reliability Analysis: A Comprehensive Approach with Continuous and Shock Deteriorations and Maintenance

Hong-Yuan Guo[1], You Dong[2], Paolo Gardoni[3] and Xiang-Lin Gu[4]

1. **Affiliation:** Department of Civil and Environmental Engineering, The Hong Kong Polytechnic University, Hong Kong, China
Key Laboratory of Performance Evolution and Control for Engineering Structures of Ministry of Education, Tongji University, 1239 Siping Rd., Shanghai 200092, China
Department of Structural Engineering, College of Civil Engineering, Tongji University, 1239 Siping Rd., Shanghai 200092, China
E-mail: 18057563r@connect.polyu.hk

2. **(Corresponding Author) Affiliation:** Department of Civil and Environmental Engineering, The Hong Kong Polytechnic University, Hong Kong, China
E-mail: you.dong@polyu.edu.hk
Tel.: +852-3400 8818

3. **Affiliation:** Department of Civil and Environmental Engineering, University of Illinois at Urbana-Champaign, Urbana, Illinois, USA
E-mail: gardoni@illinois.edu

4. **Affiliation:** Key Laboratory of Performance Evolution and Control for Engineering Structures of Ministry of Education, Tongji University, 1239 Siping Rd., Shanghai 200092, China
Department of Structural Engineering, College of Civil Engineering, Tongji University, 1239 Siping Rd., Shanghai 200092, China
E-mail: gxl@tongji.edu.cn

Abstract: Civil infrastructure may degrade due to the adverse effects of continuous damage (e.g., reinforcement corrosion) and sudden shocks (e.g., earthquakes) during its service life. Many studies have been conducted in the field of reliability-informed life-cycle assessment, but there is still a need for a general and efficient method to assess the time-dependent performance of aging structures by concerning different deterioration scenarios and maintenance actions in a unified manner. Some of the traditional methods may have difficulties in handling multiple deteriorations, nonlinear models, a large number of uncertainties, scenarios of non-differentiable performance functions, and combined effects of deterioration and maintenance. This paper develops a novel approach for time-dependent reliability analysis based on the proposed point-evolution kernel density estimation (PKDE) method and equivalent extreme performance function. The proposed approach allows consideration of various uncertainties (e.g., external loads, deterioration scenarios, maintenance models) and the associated correlation effects. In the proposed approach, both the progressive deterioration and sudden damages are considered in the modeling of the performance function. Besides, different types of maintenance schemes are assessed. The equivalent performance function is established, and the proposed PKDE method is used to address the first passage problem and non-differentiable performance function within time-dependent reliability analysis. An illustrative example is made to demonstrate the feasibility and accuracy of the proposed PKDE method. The computational results using the proposed method are verified by comparing with those from Monte Carlo simulations (MCS).

Keywords: Time-dependent reliability; Point-evolution kernel density estimation; Equivalent extreme performance function; Multiple deteriorations; Maintenance.

Introduction

The performance of civil infrastructure may degrade due to the impacts caused by aggressive environments (e.g., concrete carbonization, chloride ingress) and/or catastrophic events (e.g., hurricanes, earthquakes) (Dong *et al.* 2020; Guo *et al.* 2021; Wang *et al.* 2020). Degradation of infrastructure impairs structural resistance and safety. Therefore, maintenance actions might be needed during the infrastructure's service life. In 2019, a report from the non-profit Volcker Alliance indicated that the total maintenance cost of infrastructures in the US exceeds $1 trillion, about 5% of US GDP (Zhao *et al.* 2019). Thus, it is of great importance to assess the life-cycle performance and safety of civil infrastructure, which could help civil engineers carry out rational structural design and maintenance schemes (Barone and Frangopol 2014; Jia and Gardoni 2019a; Joanni and Rackwitz 2008).

Up to now, many approaches for life-cycle performance assessment have been developed based on probabilistic methods incorporating uncertainties in structural resistance and loading effects (Frangopol *et al.* 2017; Guo *et al.* 2020a). Initially, condition-based approaches were applied for life-cycle performance assessment (Denton 2002; Saydam *et al*. 2013; Thompson *et al*. 1998). However, it is challenging to apply condition-based methods in the identification of external load effects and quantification of structural safety. As a result, reliability-based methods were widely used to conduct comprehensive life-cycle assessments of conditions and safeties of infrastructures (Lu *et al.* 2020; Tran *et al*. 2012; Wang *et al*. 2016, 2018). However, most previous reliability-based studies focused on the single deterioration mechanism and lacked the consideration of multiple deterioration mechanisms and their possible interactions.

Therefore, Jia and Gardoni (2018a; b, 2019b) proposed a general framework of probabilistic performance and reliability analysis considering both progressive deterioration and sudden damages. Also, Kumar *et al.* (2009) developed a life-cycle assessment method for RC bridges subjected to corrosion and earthquakes. Jia and Gardoni (2019a; b) developed a stochastic life-cycle analysis and performance optimization of deteriorating systems using renewal-theory. However, most previous studies focused on the modeling of the resistance process and did not consider the correlation between the deterioration process and the load effect (Bastidas-Arteaga 2018; Kumar *et al.* 2015). Then, Wang and Zhang (2018) and Liu *et al*. (2020) proposed the use of the copula function to account for the dependence between the resistance and the external load. As a result, to date, the existing studies have achieved a comprehensive reliability analysis by considering complex deterioration mechanisms and loading effects. However, more studies should be conducted to assess the time-dependent reliability analysis by considering multiple deterioration mechanisms and the correlation between load effects and deterioration.

Though the reliability analyses of aging structures have undergone tremendous developments, most of the existing reliability-related studies do not address maintenance issues, including preventive and essential maintenance, which might limit their application in real-world engineering (Bastidas-Arteaga 2018; Stewart and Al-Harthy 2008; Wang *et al.* 2017; Wang and Zhang 2018). In the existing life-cycle maintenance, condition-based maintenance is a common strategy based on the deterioration model of a gamma process and an inspection model (Frangopol *et al.* 2004). Reliability-based maintenance is more practical than condition-based maintenance concerning the effects of loading and structural safety. Although some

previous work associated with reliability-based maintenance has been conducted (Enright and Frangopol 1999; Kong and Frangopol 2003; Kumar and Gardoni 2014), the processes of external loads were not well modeled as stochastic processes. Thus, these studies were still based on specific deterioration models, and there is still a lack of a general and robust method to comprehensively evaluate the temporal performance of aging structures under multiple deteriorations and different maintenance scenarios.

On the other hand, several reliability analysis methods have been used in the context of life-cycle performance, such as the first-order reliability method (FORM) (Frangopol *et al.* 1997), first-passage method (Sanchez-Silva *et al.* 2011; Wang *et al.* 2017), Monte Carlo simulations (MCS) (El Hassan *et al.* 2010; Zhang *et al.* 2019), and renewal-theory (Jia and Gardoni 2019b). However, although FORM and first-passage method can be efficiently applied in specific scenarios, it is still necessary to use MCS to conduct reliability analysis for complex scenarios involving multiple deteriorations and nonlinear modes (Akiyama et al. 2019; Jia and Gardoni 2018a). Due to the inefficiency and computational burden of classical MCS, some studies have been undertaken to improve the computational efficiency of specific scenarios (e.g., importance sampling, (Au and Beck 2003; Jia and Gardoni 2018a) or semi-sampling semi-analytical methods (Kumar *et al.* 2015; Kumar and Gardoni 2014; Wang *et al.* 2017). However, these case-specific improvements may not be as generally applicable as traditional MCS. Thus, it is of great significance to develop a novel and general method for time-dependent reliability analysis. In the past decades, several methods based on the probability density function (PDF) have been proposed to perform reliability analysis by estimating a target PDF. For example, Li

and Chen (2009) proposed a probability density evolution method (PDEM) for reliability analysis by solving the generalized density evolution equation (GDEE). However, PDEM relies on the establishment and computation of GDEE, and it is challenging to build and solve GDEE. The PDEM cannot be directly used to solve the cases of the non-differentiable performance function (Guo *et al.* 2020b). Thus, the applicability of PDEM might be limited, and there is a need to propose a new method for PDF oriented analysis to avoid solving GDEE. On the other hand, some nonparametric evaluation approaches, such as the kernel density estimation method (KDEM), are applied to assess the target PDF (Colbrook *et al.* 2020; Jia *et al.* 2017a; Sheather and Jones 1991; Silverman 1986). Existing studies related to KDEM focused on the optimal selection of bandwidth for KDEM. For instance, Botev *et al.* (2010) suggested an adaptive bandwidth selector through the smoothing property of the linear diffusion process. Besides, Alibrandi and Mosalam (2018) developed a KDEM based on the principle of maximum entropy to estimate the long-tailed distribution from a small number of samples. However, classical KDEMs are mostly based on the idea of MCS, where each sample is equally weighted. Thus, the accuracy of classical KDEMs is highly dependent on the sampling number. In this paper, the point-evolution method is applied to reduce the sampling number in KDEM. To the best knowledge of the authors, there have been no studies focusing on the application of KDEM within the time-dependent reliability analysis by incorporating the point-evolution method.

Therefore, this study develops a point-evolution kernel density estimation (PKDE) based framework for time-dependent reliability analysis by considering multiple deterioration mechanisms, the correlation between load effects and deterioration, and maintenance schemes.

The proposed PKDE can improve the computational efficiency of the reliability analysis. The "Time-Dependent Performance Function with Multiple Deteriorations and Maintenance Action" section introduces the concepts of the proposed framework. The "PDF oriented Reliability Analysis" section reviews the classical PDEM and KDEM, describes the proposed PKDE in detail, and compares the algorithms of the three PDF-oriented methods. Then, in the "Illustrative Example" section, the feasibility and accuracy of the framework are demonstrated using an example. Meanwhile, different maintenance schemes and their influences on reliability are investigated. Also, the results of the reliability analysis are compared with other methods. Finally, conclusions are drawn, and future work is pointed out.

Time-Dependent Performance Function with Multiple Deteriorations and Maintenance Action

Over the life of an engineering system, it may undergo multiple deteriorations. To estimate the stochastic performance of the system, it is necessary to assess its time-dependent capacity and demand (Jia and Gardoni 2018a, 2019a; b; Kumar *et al.* 2015). Therefore, in this study, a performance function involving the capacity and demand of a degrading engineering system under multiple deterioration scenarios is introduced. Meanwhile, the effect of maintenance action on performance action is also discussed, as shown in **Fig.1**.

Given the random total input variables $\boldsymbol{\Theta} = [\Theta_1, \Theta_2, \ldots, \Theta_s]$ (s is the number of variables), the performance function $G(\boldsymbol{\Theta}, t)$ at time t is defined as

$$G\left(\boldsymbol{\Theta}, t\right) = R\left(\boldsymbol{\Theta}_R, t\right) - S\left(\boldsymbol{\Theta}_S, t\right) \tag{1}$$

where $R(\boldsymbol{\Theta}_R, t)$ and $S(\boldsymbol{\Theta}_S, t)$ are the stochastic processes of instantaneous resistance R and load

157 effect S, in which $\boldsymbol{\Theta}_R$ and $\boldsymbol{\Theta}_S$ are the random input variables of R and S, respectively ($\boldsymbol{\Theta} = [\boldsymbol{\Theta}_R,$

158 $\boldsymbol{\Theta}_S]$). For $S(\boldsymbol{\Theta}_S, t)$, it consists of dead load $S_d(\boldsymbol{\Theta}_{Sd})$ and live load $S_l(\boldsymbol{\Theta}_{Sl}, t)$.

159 $$S\left(\boldsymbol{\Theta}_S, t\right) = S_d\left(\boldsymbol{\Theta}_{S_d}\right) + S_l\left(\boldsymbol{\Theta}_{S_l}, t\right) \tag{2}$$

160 where $\boldsymbol{\Theta}_{Sd}$ and $\boldsymbol{\Theta}_{Sl}$ are the random input variables of S_d and S_l, respectively ($\boldsymbol{\Theta}_S = [\boldsymbol{\Theta}_{Sd}, \boldsymbol{\Theta}_{Sl}]$).

161 In previous studies, the dependence between deterioration and the occurrence of stochastic

162 loads was usually ignored (Kumar *et al.* 2015). In practice, stochastic loads not only cause

163 demands for the engineering system but may also lead to shock deterioration (Jia and Gardoni

164 2018a).

165 Concerning both the progressive deterioration and shock deterioration caused by external

166 loads, the resistance function R ($\boldsymbol{\Theta}_R$, t) is described by a model as

167 $$R\left(\boldsymbol{\Theta}_R, t\right) = R_0 - D_P\left(\boldsymbol{\Theta}_{D_p}, t\right) - D_S\left(\boldsymbol{\Theta}_{D_s}, t\right) \tag{3}$$

168 where R_0 is the random initial resistance; D_P ($\boldsymbol{\Theta}_{Dp}$, t) and D_S ($\boldsymbol{\Theta}_{Ds}$, t) are the damages due to

169 the progressive deterioration and shock deterioration, respectively; and $\boldsymbol{\Theta}_{Dp}$ and $\boldsymbol{\Theta}_{Ds}$ are the

170 random input variables of D_P and D_S, respectively ($\boldsymbol{\Theta}_R = [R_0, \boldsymbol{\Theta}_{Dp}, \boldsymbol{\Theta}_{Ds}]$).

171 For the modeling of D_P ($\boldsymbol{\Theta}_{Dp}$, t), Kumar *et al.* (2015) proposed to use a combination of

172 deterministic functions to model progressive deterioration, and Jia and Gardoni (2018a)

173 suggested a nonhomogeneous state-dependent Markov process model that considers

174 uncertainties and time-dependent deterioration process. For D_S ($\boldsymbol{\Theta}_{Ds}$, t), the characteristics of

175 the shock, such as the occurrence rate and intensity, should be modeled. A stochastic model,

176 such as the Poisson process, either homogeneous or nonhomogeneous, was usually applied to

177 model the shock occurrence (Jia and Gardoni 2019b; Kumar *et al.* 2015). Since Eq. (3) does

not require specifying the format of deterioration models, the forms of progressive and shock deterioration are not identified in Eq.(3). As long as the damages caused by progressive and shock deterioration can be quantified, the performance function could be built and the proposed framework could be implemented. In general, given the performance function, the performance of the investigated engineering structure can be assessed.

The performance function can be improved by maintenance actions. In this study, the relevant maintenance actions are determined through a time-varying performance indicator, i.e., the time-varying reliability index β (Jia *et al.* 2017b). Given the relevant threshold (e.g., β_{c1} and β_{c2}), the timing for different maintenance types can be determined. The i-th maintenance time instants of preventive maintenance and essential maintenance are denoted as $t_{p,i}$ (i = 1, 2, …, n_p) and $t_{e,i}$ (i = 1, 2, …, n_e), respectively, where n_p and n_e are the numbers of preventive maintenance and essential maintenance. As an illustration, in **Fig. 2**, the solid line, dotted, dashed, and dot-dash lines denote the β associated with no maintenance, replacement, enhancement, and preventive maintenance & replacement, respectively. If no maintenance is applied, β decreases continuously with time and the initial β is supposed to be β_0. Concerning the scenario of preventive maintenance & replacement, when β reaches the threshold value β_{c1}, the first preventive maintenance is initiated and the corresponding time is denoted as $t_{p,1}$. Furthermore, when β further reaches the threshold value β_{c2}, the first essential maintenance, i.e., replacement, is activated and the corresponding time is denoted as $t_{e,1}$. After performing replacement, the investigated structure would be fully recovered and β returns to β_0. Then, another preventive maintenance occurs once β reaches the threshold value β_{c1} again, and the

corresponding time instant is denoted as $t_{p,2}$. Besides, concerning the scenarios of replacement and enhancement, $t_{e,1}$ and $t_{e,2}$ are the first and second-time instants, when the β reaches the threshold value β_{c2}, and corresponding essential maintenance can be performed, where enhancement could increase the β after essential maintenance.

The effect of different maintenance actions (i.e., preventative, replacement, and enhancement) is introduced as follows:

Concerning the changing rate of the performance function after preventive maintenance, a factor φ (<1) is introduced to consider the effect of preventive maintenance actions on the time-variant structural performance. Given the detailed information of preventive maintenance action, the value of φ can be determined. The performance function after preventive maintenance could be updated as $R^*(\boldsymbol{\Theta}_R, t)$:

$$\begin{aligned} R^*(\boldsymbol{\Theta}_R, t) &= R_0 - D_P^*\left(\boldsymbol{\Theta}_P, t\right) - D_S\left(\boldsymbol{\Theta}_S, t\right) \\ &= R_0 - \varphi \cdot D_P\left(\boldsymbol{\Theta}_P, t\right) - D_S\left(\boldsymbol{\Theta}_S, t\right), \\ t \in (t_{p,i}, +\infty) \ or \ t \in (t_{p,i}, t_{e,j}], i &= 1,2,..., j = 1,2,..., t_{p,i} < t_{e,j} \end{aligned} \tag{4}$$

where $t_{n,i}$ is the i-th time instant when β is reduced to β_{c1}; $(t_{p,i}, +\infty)$ (i = 1, 2,…) is the time interval between the i-th preventive maintenance and end of service life; and $(t_{p,i}, t_{e,j}]$ (j = 1, 2,….) is the time interval between the i-th preventive maintenance and the j-th essential maintenance. In this study, a preventive maintenance is assumed to be effective until the next essential maintenance. If no essential maintenance is applied, the preventive maintenance is assumed to be effective until the end of the service life.

Besides, when β is reduced to β_{c2} at the time $t_{e,i}$ and replacement occurs, the structural resistance $R^*(\boldsymbol{\Theta}_R, t)$ can be updated to the initial value, which can be expressed as

$$R^*(\boldsymbol{\Theta}_R, t) = R\left(\boldsymbol{\Theta}_R, t - t_{e,i}\right), \quad t \in (t_{e,i}, +\infty), t \in (t_{e,i}, t_{e,i+1}], i = 1, 2, \ldots \tag{5}$$

where $(t_{e,i}, +\infty)$ (i = 1, 2,…) is the time interval between i-th essential maintenance and end of service life; and $(t_{e,i}, t_{e,i+1}]$ (j = 1, 2,….) denotes the time interval between the i-th essential maintenance and the (i+1)-th essential maintenance. For enhancement as indicated in **Fig. 2**, the structural resistance is enhanced and exceeds the initial value where the increased value is denoted as R_{en} and $R^*(\boldsymbol{\Theta}_R, t)$ can be computed as:

$$R^*(\boldsymbol{\Theta}_R, t) = R\left(\boldsymbol{\Theta}_R, t - t_{e,i}\right) + R_{en}, \quad t \in (t_{e,i}, +\infty), t \in (t_{e,i}, t_{e,i+1}], i = 1, 2, \ldots \tag{6}$$

where R_{en} is the value of performance enhancement (0 for replacement).

On the other hand, denoting external load and shock deterioration at time t as $S_{l,t}$ and $D_{S,t}$, a copula function (e.g., Gaussian) can be employed to consider the correlation between $S_{l,t}$ and $D_{S,t}$ at time t with marginal cumulative density functions (CDFs) of $F_{Sl,t}$ and $F_{Ds,t}$, respectively (Wang *et al.* 2017):

$$F_{S_{l,t}, D_{S,t}}\left(S_{l,t}, D_{S,t}\right) = \Phi_G\left[\Phi^{-1}\left(F_{S_{l,t}}\left(S_{l,t}\right)\right), \Phi^{-1}\left(F_{D_{S,t}}\left(D_{S,t}\right)\right)\right] \tag{7}$$

where $F_{Sl,t,Ds,t}$ is the joint CDF of ($S_{l,t}$, $D_{S,t}$); Φ_G is the joint CDF of a multivariate standard normal distribution; and Φ^{-1} is the inverse cumulative distribution function (CDF) of standard normal distribution.

After modeling the resistance and external load, the failure probability $P_f(t)$ and reliability index $\beta(t)$ at time t can be evaluated. In general, the estimation of $P_f(t)$ and $\beta(t)$ depends on their definitions. For instance, ignoring the temporal correlation of $G(\boldsymbol{\Theta}, t)$ and supposing that no essential maintenance is applied, $P_f(t)$ can be defined as the probability that $G(\boldsymbol{\Theta}, t)$ is below

zero:

$$P_f(t) = P\left(G(\boldsymbol{\Theta}, t) < 0\right) \tag{8}$$

Then, $\beta(t)$ can be calculated through $P_f(t)$ as (Ditlevsen and Madsen 1996):

$$\beta(t) = \Phi^{-1}\left(1 - P_f(t)\right) \tag{9}$$

However, such a definition cannot take into account the first passage problem and may underestimate the failure probability. Thus, a rigorous definition of $P_f(t)$ can be written as (Lutes and Sarkani 2004):

$$P_f(t) = P\left(G(\boldsymbol{\Theta}, \tau) < 0, \exists\, \tau \in [0, t]\right) \tag{10}$$

Regarding the first passage problem, some strategies like up-crossing rate methods (Hu and Du 2013; Li and Melchers 2005), outcrossing rate methods (Andrieu-Renaud *et al.* 2004; Sudret 2008), and MCS methods (Gu *et al.* 2018; Tu *et al.* 2017) have been employed in previous studies. The former two methods might be limited by the adopted models associated with resistance and load effect and are hard to be employed in the scenarios of multiple deterioration mechanisms. Although the latter one could avoid the mathematical difficulties in reliability estimation, it might cause a substantial computational burden. Besides, if essential maintenances are applied, the resistance $R(\boldsymbol{\Theta}_R, t)$ would increase, but the $P_f(t)$ and $\beta(t)$ calculated by Eqs.(10) and (9) would remain unchanged. To ensure the reliability returns to or exceed the initial status after the essential maintenance, $P_f(t)$ should be redefined as:

$$P_f(t) = P\left(G(\boldsymbol{\Theta}, \tau) < 0, \exists\, \tau \in (t_{e,i}, t]\right), t \in (t_{e,i}, t_{e,i+1}], i = 1, 2, \ldots \tag{11}$$

Thus, being different from the traditional first passage problem, the probabilistic information that was in the failure domain could return to the safety domain after the implementation of essential maintenance. With respect to generality and computational

efficiency in reliability analysis, conventional methods might not be appropriate and a more flexible reliability analysis method should be adopted.

PDF oriented Reliability Analysis

The main thought of PDF oriented reliability analysis is to calculate $P_f(t)$ by the integration of the PDF of performance function:

$$P_f(t) = \int_{g<0} p_G(g,t)\mathrm{d}g \tag{12}$$

in which $p_G(g, t)$ is the PDF of the performance function. Thus, the main objective of PDF oriented method is to perform the reliability analysis by capturing the time-dependent PDFs of the performance functions.

To obtain $p_G(g, t)$, Li and Chen (2008, 2009, 2014) proposed a probability density evolution method (PDEM), which initially aims at performing the dynamic reliability of nonlinear structures. In terms of a series of mathematical derivations, the generalized density evolution equation (GDEE) can be obtained as follows:

$$\frac{\partial p_{G\boldsymbol{\Theta}}(g,\boldsymbol{\theta},t)}{\partial t} + \dot{G}(\boldsymbol{\Theta},t)\frac{\partial p_{G\boldsymbol{\Theta}}(g,\boldsymbol{\theta},t)}{\partial g} = 0 \tag{13}$$

where $p_{G\boldsymbol{\Theta}}(g, \boldsymbol{\theta}, t)$ denotes the joint PDF of G and $\boldsymbol{\Theta}$ at time t. Besides, the boundary condition and analytical solution of Eq.(13) can be written as:

$$\begin{aligned} p_{G\Theta}(g,\boldsymbol{\theta},0) &= \delta[g - G(\boldsymbol{\Theta},0)]p_{\boldsymbol{\Theta}}(\boldsymbol{\theta}), \\ p_{G\Theta}(g,\boldsymbol{\theta},t) &= \delta[g - G(\boldsymbol{\Theta},t)]p_{\boldsymbol{\Theta}}(\boldsymbol{\theta}) \end{aligned} \tag{14}$$

in which $p_{\boldsymbol{\Theta}}(\boldsymbol{\theta})$ denotes the joint PDF of random vector $\boldsymbol{\Theta}$ and $\delta(\cdot)$ is Dirac's delta function. Since the closed-form solution of Eq.(13) is difficult to obtain, the total variation diminishing (TVD) scheme-based finite difference method (FDM) can be used to solve it (Li *et al.* 2012; Li

281 and Chen 2009). Regarding FDM, the first step is to choose appropriate time step Δt and space
282 step Δg and build the difference grid, in which Δt and Δg are subjected to Courant-Friedrichs-
283 Lewy (CFL) condition (Courant *et al.* 1928).

284 $$\left|\frac{\Delta t}{\Delta g} v\right| \leq 1 \tag{15}$$

285 where v is the derivative function of the sampled performance function which limits the
286 selection of Δt and Δg. Then, $p_G(g, t)$ could be computed by integrating out $\boldsymbol{\Theta}$ (e.g., by
287 consistency rule) (Ang and Tang 2007):

288 $$p_G(g,t) = \int_{\Omega_{\boldsymbol{\Theta}}} p_{G\boldsymbol{\Theta}}(g,\boldsymbol{\theta},t)\, \mathrm{d}\boldsymbol{\theta} \tag{16}$$

289 Regarding the first-passage problem and the scenario of no maintenance, an absorbing
290 boundary condition needs to be imposed, which means that a representative point that comes to
291 the failure zone will not return to the safety zone. By employing an absorption boundary, some
292 probabilistic information of $p_G(g, t)$ will be lost due to the failure representation points. The
293 updated $p_G(g, t)$ can be denoted as the residual PDF, $p^*_G(g, t)$, and computed using Eq.(17).

294 $$p_G^*(g,t) \equiv \left\{ p_G(g,t)|_{g<0} = 0 \right\} \tag{17}$$

295 Then, $P_f(t)$ could be solved through the integration of $p^*_G(g, t)$ as in Eq.(18).

296 $$P_f(t) = 1 - \int_0^{+\infty} p_G^*(g,t)\mathrm{d}g \tag{18}$$

297 Besides, $P_f(t)$ can be calculated by Eq. (18) for preventive maintenance, though a reduced
298 deterioration rate brings the reduction of the changing rate of $\beta(t)$. However, for essential
299 maintenance, $R(\boldsymbol{\Theta}_R, t)$ and the PDF of performance function are updated when $\beta(t)$ is reduced
300 to β_{c2}. Regarding the absorbing boundary condition, once a sample fails, the associated
301 probability does never return to the safety domain (Li and Chen 2009). Thus, although $R(\boldsymbol{\Theta}_R, t)$
302 can be updated after repair actions, $\beta(t)$ does not increase and becomes a non-increasing

function. Thus, this method cannot be used to solve the time-dependent reliability by considering the effect of maintenance action.

Equivalent extreme performance function

For the first-passage problem and the maintenance effect, absorbing boundary condition seems unpractical, and then a more general approach is developed to build an equivalent extreme performance function g^* as indicated in Eq.(19) and **Fig. 3**. In **Fig. 3**, it can be found that in each interval $[0, t_{e,1})$, $[t_{e,1}, t_{e,2})$, and $[t_{e,2}, +\infty)$, the original performance function g is fluctuating but g^* is a nonincreasing function. Due to the monotonic nature of g^*, there exists no difficulty in solving the first-passage problem, and time-dependent reliability can be handled similarly to Eq.(12). Thus, $P_f(t)$ can be calculated through the integration of the PDF of g^*, $p_{G^*}(g^*,t)$, via Eq.(20).

$$g^* = G^*(\boldsymbol{\Theta}, t) = \min\left\{G(\boldsymbol{\Theta}, \tau), \tau \in (t_{e,i}, t]\right\}, t \in (t_{e,i}, t_{e,i+1}], i = 1, 2, \ldots \tag{19}$$

$$P_f(t) = \int_{g^*<0} p_{G^*}\left(g^*, t\right) \mathrm{d}g^* \tag{20}$$

Besides, Eq.(19) can also be applied to the scenarios of no maintenance or preventive maintenance if $t_{n,i}$ is assumed as zero, which indicates that the equivalent extreme performance function is appropriate for all scenarios. However, the $\min\{\cdot\}$ in Eq.(19) is an abstract function so that $p_{G^*}(g^*,t)$ is not a differentiable function and the GDEE of g^* is unavailable. Similar phenomena usually occur in time-dependent systems, such as the structural resistance suffering from sudden damage and the performance function subjected to the stochastic loading process. According to CFL condition Eq. (15), dramatic changes in the performance function will severely limit the choice of Δg and Δt reducing the accuracy of the FDM, further compromising

the accuracy of PDEM analysis (Guo *et al.* 2020b), which might make it challenging to perform PDF-oriented analysis. Therefore, the current PDEM cannot be widely used within the life-cycle assessment process. Particularly, it may not be appropriate to apply PDEM in the scenario with equivalent extreme performance function due to the difficulty in obtaining PDF via GDEE. Therefore, in this study, instead of establishing and solving GDEE as PDEM, the nonparametric density estimation method would be adopted to evaluate the PDF. More detailed information can be found in the following section.

Kernel density estimation-based method (KDEM)

The main demerit of PDEM is that a differentiable performance function should be established. In this study, an alternative strategy for capturing PDFs is to apply a nonparametric density estimation method to evaluate the PDF directly without capturing the differentiable function. Such a method is called kernel density estimation (KDE), and the basic idea is to evaluate the target PDF through a series of samples and kernel density estimators (Silverman 1986). Regarding the target PDF $f(x)$, its estimation $\hat{f}(x,h)$ can be written as

$$\hat{f}(x,h) = 1/M \cdot \sum_{i=1}^{M} K(x, x_i, h) \tag{21}$$

where x_i is the i-th sample; M and h are the number of samples and the bandwidth; and K is the kernel function, which could be selected according to the distribution region and characteristics of samples (Alibrandi and Ricciardi 2008; Rawa *et al.* 2011). For instance, if the target distribution is an infinite region, i.e., $x \in (-\infty, +\infty)$, K could be the PDF of a Gaussian distribution whose mean is the value of sample x_i and the standard deviation is h

$$K(x, x_i, h) = \frac{1}{h\sqrt{2\pi}} \exp\left[-\frac{1}{2}\left(\frac{x - x_i}{h} \right)^2 \right] \tag{22}$$

Moreover, for finite regions, such as $x \in [a, b]$, the kernel function could be a beta distribution; for semi-bounded region, i.e., $x \in [0, +\infty)$, the kernel function could be a lognormal or gamma distributions. Besides, if h is infinitely close to 0, the kernel function becomes $\delta(\cdot)$, and if M is close to infinity, $\hat{f}(x, h)$ becomes infinitely close to $f(x)$.

Thus, employing the KDEM in time-dependent reliability analysis, the PDF of the equivalent extreme performance function G^* at time t, $p_{G^*}(g^*, t)$, can be estimated as

$$\hat{p}_{G^*}(g^*, t) = \sum_{i=1}^{M} \frac{1}{M} K(g, G^*(\boldsymbol{\theta}_i, t), h) \tag{23}$$

However, in most cases, it is not possible to apply a large number of samples due to the limitations of experimental conditions and computational burden. Then, a common problem for KDE is to select an appropriate bandwidth h based on a limited number of samples. In general, the optimal bandwidth h is determined based on the criterion of mean integrated square error (MISE), which can be decomposed into integrated squared bias and integrated variance components. $\hat{f}(x, h)$ denotes the estimator of $f(x)$ for a given h. Since $f(x)$ is unknown, it is difficult to obtain the h satisfying the minimum of MISE. If the target distribution is close to a Gaussian distribution, and the kernel is chosen as a Gaussian kernel, the choice of h could be determined according to Silverman's optimum bandwidth h (Silverman 1986):

$$h = \hat{\sigma}\left(4 / (3M)\right)^{0.2} \tag{24}$$

where $\hat{\sigma}$ is the sample standard deviation. If the target distribution is far from a Gaussian distribution, Eq.(24) might cause the inaccurate results of KDE. Thus, to obtain the appropriate

bandwidth, Botev *et al.* (2010) proposed a plug-in bandwidth selection method based on the Sheather-Jones algorithm (more details refer to Appendix A). Although Botev's approach suggests a practical way to obtain the appropriate bandwidth, the accuracy of such a method still strongly relies on the randomly sampled data. Essentially, it is still a MCS-based method that requires a large amount of sampling. To overcome this demerit and increase the computational efficiency, the PKDE is proposed in the following section.

Point-evolution kernel density estimation

As mentioned earlier, in PDEM, there is no need to generate as many samples as in MCS, but rather there is a need to select representative points by the point-evolution method. However, for PDEM, the target PDF must be solved by computing the GDEE. For KDEM, the target PDF can be captured using KDE without solving the GDEE, but a large amount of sampling is required. Therefore, a new method of point-evolution kernel density estimation (PKDE) is proposed to combine the ideas and merits of classical KDE and PDEM to evaluate the target PDF.

The main idea of PKDE is to apply the point-evolution method for the selection of representative points and then evaluate the PDFs by means of kernel density estimators. The principal idea of the point-evolution method is to partition the random space into n_{sel} subdomains through selecting representative points (Chen *et al.* 2009). In general, a low-discrepancy sequence, such as the number-theoretical method (NTM) (Li and Chen 2007) or Sobol sequence (Radović *et al.* 1996), can be used to generate a uniform point set $\mathbf{K}$. Then, $\mathbf{K}$ will be transformed into target point set $\boldsymbol{\Theta}$ in terms of its marginal input distribution where each

target point $\theta_{w,i}$ (the w-th random variable and i-th representative point) is written as:

$$\theta_{w,i} = F_w^{-1}\left(\kappa_{w,i}\right), w = 1,2,...,s, i = 1,2,...,n_{sel} \tag{25}$$

in which $F_w^{-1}(\cdot)$ denotes the inverse cumulative distribution function (CDF) of the w-th random variable in $\boldsymbol{\Theta}$. Then, the point set can be further improved, and the new point $\theta'_{w,j}$ could express as (Chen *et al.* 2016).

$$\theta'_{w,j} = F_w^{-1}\left\{\sum_{i=1}^{n_{sel}} P_{a,i} \cdot I\{\theta_{w,i} < \theta_{w,j}\} + 0.5P_{a,j}\right\} \tag{26}$$

where $I\{\cdot\}$ is the indicator function that $I\{\cdot\} = 1$ if the condition in $\{\cdot\}$ is satisfied and $P_{a,i}$ is the assigned probability of i-th representative point calculated by integrating $p_{\boldsymbol{\Theta}}(\boldsymbol{\theta})$ over the region of V_i

$$P_{a,i} = \Pr\{\boldsymbol{\Theta} \in V_i\} = \int_{V_i} p_{\boldsymbol{\Theta}}(\boldsymbol{\theta})\, \mathrm{d}\boldsymbol{\theta}, a = 1,2,...,n_{sel} \tag{27}$$

where V_i denotes the volume of Voronoi cell of the random space of i-th representative point (Chen and Zhang 2013).

Then, according to the point-evolution method, the estimation of target PDF can be expressed as the sum of a series of representative points with assigned probabilities:

$$\hat{f}\left(x\right) = \sum_{i=1}^{M} P_{a,i}\delta\left(x - x_i\right) \tag{28}$$

In PKDE, δ in Eq.(28) is estimated through a kernel density estimator. Comparing Eq.(28) with Eq.(21), the difference between KDE and PKDE is that $1/M$ is replaced by the assigned probability $P_{a,i}$. Then, the estimation of the target PDF can be rewritten as follows:

$$\hat{f}\left(x,h\right) = \sum_{i=1}^{M} P_{a,i}K\left(x, x_i, h\right) \tag{29}$$

where $K(\cdot)$ is the kernel function that can be selected according to the "Kernel density

estimation-based method (KDEM)" subsection; and h is the bandwidth that can be evaluated by Botev's approach. However, concerning the influences of assigned probability $P_{a,i}$ on the selection of optimal bandwidth, the initial boundary condition of Eq.(A-1) is revised as

$$\hat{f}(x,0) \approx \sum_{i=1}^{M} P_{a,i} \cdot H\left(\Delta x - \left|x - x_i\right|\right) \tag{30}$$

in which Δx is an extremely small value and $H(y)$ is a Heaviside function that equals 1 if y is not less than 0, otherwise, it equals 0. For the Gaussian kernel function, the optimal estimation of h can be obtained by solving Eq.(A-4).

To demonstrate the efficiency and accuracy of the proposed PKDE, two simple cases are made to evaluate the PDFs of x_1 and x_2:

$$x_1 = \theta_1^2 + \theta_2, x_2 = \theta_1 \cdot H\left(\left|\theta_1\right| - \left|\theta_3\right|\right) + \theta_3 \cdot \left(1 - H\left(\left|\theta_1\right| - \left|\theta_3\right|\right)\right) \tag{31}$$

where θ_1, θ_2, and θ_3 follow $N(-2,1)$, $N(1,3)$, and $N(2,3)$, respectively; and $H(\cdot)$ is a Heaviside function which equals one if the value in parentheses is not less than 0, otherwise equals 0.

An illustrative example is introduced here to demonstrate the feasibility and efficiency of the proposed method. By employing a Gaussian kernel, the PDFs of x_1 and x_2 are evaluated through different methods: 10^6 times sampling from Botev's KDEM, 256 times sampling from Silverman's KDEM, Botev's KDEM, and the proposed PKDE. The samples of the former three methods are generated by brute MCS, but the last one is based on the Sobol sequence (Radović *et al.* 1996).

Comparisons of the estimation results for the two cases are shown in **Fig. 4**. It can be found that, both in **Figs.4a** and **b**, the PDF from 10^6 times sampling from Botev's KDEM is close to the proposed PKDE but quite different from others. Besides, in both **Figs.4a** and **b**, subgraphs

426 are plotted in log scale to magnify the tail of the negative portion of the PDFs. Although the
427 subgraphs in **Fig. 4** show that the tail distribution of PKDE slightly deviates on the negative
428 axis, the proposed PKDE can basically provide well-estimated tails of the PDF. Accuracy of the
429 tails of the PDF is crucial for reliability analysis as the modeling of PDF tails generally
430 determines the accuracy of the reliability results. Therefore, the proposed PKDE exhibits
431 significant effects regardless of whether it is a Gaussian-like or multi-peak distribution. These
432 results show the feasibility and accuracy of the proposed PKDE.

433 On the other hand, regarding time-dependent reliability analysis, PKDE should be applied
434 based on the value of performance function for each representative point at each time instant.
435 Moreover, considering the first passage problem, the PDF of the equivalent extreme
436 performance function at time t $p_{G^*}(g^*,t)$ can be estimated as

437 $$\hat{p}_{G^*}\left(g^*,t\right)=\sum_{i=1}^{M}P_{a,i}K\left(g,G^*(\boldsymbol{\theta}_i,t),h\right) \tag{32}$$

438 Comparing with PDEM, $\hat{p}_{G^*}\left(g^*,t\right)$ can be easily and efficiently obtained by Eq.(32)
439 without the process of FDM and absorbing boundary condition. Therefore, the proposed PKDE
440 can be flexibly applied in the time-dependent reliability analysis of aging structures, especially
441 for the scenarios with different deterioration scenarios and maintenance actions within the
442 service life.

443 The main algorithms of the proposed reliability analysis framework, including PDEM,
444 KDEM, and PKDE, are briefly summarized in Algorithm 1. The main inputs of the algorithms
445 are the name of applied method ‘method’, the number of representative points or samples N_{sel},
446 the random variables $\boldsymbol{\Theta}$ (dimension s), the performance function $G(\boldsymbol{\Theta}, t)$, the time period [0,

447 T_{tot}] and the time interval dt; and the outputs are time-dependent reliability index $\beta(t)$ and failure
448 probability P_f (t). The fundamental difference between those three methods is the process of
449 capturing the target PDF of performance function. For PDEM, the main steps are: generating
450 N_{sel} representative points, calculating the assigned probability of each representative point, then
451 capturing PDF through FDM. For KDEM, the main steps are: generating N_{sel} samples,
452 assessing the optimal bandwidth through Botev's approach, and then estimating the target PDF
453 through Eq.(23). For the proposed PKDE, the N_{sel} representative points are selected, optimal
454 bandwidth is also evaluated through Botev's approach, and then estimating the target PDF
455 through Eq.(29). Once the target PDF is captured, P_f (t) could be obtained by integrating the
456 PDF.
457

Algorithm 1. PDF oriented Reliability Analysis including three methods

Switch (method):
Case 'PDEM'
    Generate N_{sel} representative points via Sobol Sequences
    for i=1: N_{sel} **do**
        for t=1: dt : T_{tot} **do**
            Solve i-th $p^i{}_G(g,t)$ through finite difference
            Set the absorbing boundary condition $p^i{}_G(g, t)|_{g<0}=0$ to obtain $p^i{}_{G^*}(g^*, t)$
        end do
    end do
    Sum all $p^i{}_{G^*}(g^*, t)$ to obtain $p_{G^*}(g^*, t)$
    Calculate the P_f (t) through $1-\int_0^{+\infty} p_G^*(g,t)dg$ and $\beta(t)=\Phi(1\text{-}P_f(t))$
Case 'KDEM'
    Generate N_{sel} random samples
    for t=1: dt : T_{tot} **do**
        Set initial error variable ε0 = 1e3, precision ε, initial z_0 = ε, n = 0 and initial guess h = 0
        while $\varepsilon_0 > \varepsilon$ **do**
            Set $z_{n+1}=\xi\gamma^{[l]}(z_n)$
            $\varepsilon_0=|z_{n+1}\text{-}\ z_n|$, and n: = n+1
        end do
        Obtain the optimal bandwidth $h=\sqrt{z_{n+1}}$ and $p_G{}^*(g^*,t)$ through Eq.(23)
        Calculate the P_f (t) through $\int_{-\infty}^{0} p_{G^*}(g^*,t)dg^*$ and $\beta(t)=\Phi(1\text{-}P_f(t))$
    end do

Case 'PKDE'
    Generate N_{sel} representive points via Sobol Sequences
    for i=1: N_{sel} **do**
        Compute the assigned probability of *i*-th representative point $P_{a,i}$
    end do
    for *t*=1: d*t* : T_{tot} **do**
        Set initial error variable $\varepsilon_0 = 10^3$, precision ε, initial $z_0 = \varepsilon$, $n = 0$ and initial guess $h = 0$
        while $\varepsilon_0 > \varepsilon$ **do**
            Set $z_{n+1}=\xi\gamma^{[l]}(z_n)$
            $\varepsilon 0=| z_{n+1}- z_n|$, and n:= n+1
        end do
        Obtain the optimal bandwidth $h = \sqrt{z_{n+1}}$ and $p_{G^*}(g^*,t)$ through Eq.(29)
        Calculate the $P_f(t)$ through $\int_{-\infty}^{0} p_{G^*}(g^*,t)dg^*$ and $\beta(t)=\Phi(1-P_f(t))$
    end do

Illustrative Example

This section presents numerical example to illustrate the feasibility and capability of the proposed method. Both progressive and sudden damage are considered in the resistance model, while the load model is associated with both dead and live loads. Also, different maintenance schemes and their effects on structural performance are investigated.

Time-dependent resistance and load effect

To conduct a reliability analysis, the first step is to model the resistance and load effect. Consider a structure subjected to dead load S_d, live load S_l, progressive deterioration, and S_l induced sudden damage with a service life of 40 years. In this case, S_d is assumed as a lognormal distributed random variable with mean value μ_d and coefficient of variation (COV) δ_d; and S_l is modeled by a stationary Poisson process with a mean occurrence rate of λ. Denoting the occurrence times of load event within t years as $m(t)$, the probability that k times of load events occur is

$$\mathrm{P}\left(m(t)=k\right)=\frac{\left(\int_0^t \lambda dt\right)^k \exp\left(-\int_0^t \lambda dt\right)}{k!}, k=0,1,2,... \tag{33}$$

The intensity of each live load event follows Gumbel distribution (Wang *et al.* 2017). The mean value and COV are denoted as μ_l and δ_l.

The progressive deterioration is modeled by a function of time and a random variable of initial capacity for illustrative purposes, while shock deterioration is represented by the sum of a series of independent random variables. Besides, the shock deterioration and live load event are assumed to occur simultaneously, and then the resistance function is written as:

$$R(t)=R_0 \cdot d(t)-\sum_{i=m_i+1}^{m(t)} \Delta D_{sk,i} \tag{34}$$

where R_0 follows a lognormal distribution with the mean value μ_{R0} and COV δ_{R0}; $\Delta D_{\mathrm{sk},i}$ is the i-th shock deterioration following the lognormal distribution whose mean value and COV are μ_{sk} and δ_{sk}; m_{i} is equal to 0, if no essential maintenance is applied, or the number of sudden damage when essential maintenance is applied; and $d(t)$ is the progressive deterioration function which is assumed as (Mori and Ellingwood 1993)

$$d(t)=1-a \cdot t^b \tag{35}$$

where a and b are the shape parameters of the progressive deterioration function. Concerning the correlation between $\Delta D_{\mathrm{sk},i}$ and $\mathrm{S}_{l,i}$ (i-th live load event), $\Delta D_{\mathrm{sk},i}$ and $\mathrm{S}_{l,i}$ are converted into correlated standard normal variables U_1 and U_2 through

$$F_{S_{l,i}}\left(S_{l,i}\right)=\Phi\left(U_1\right), F_{D_{sk,i}}\left(D_{sk,i}\right)=\Phi\left(U_2\right) \tag{36}$$

The correlation coefficient matrix of (U_1, U_2) is denoted as Ψ_i:

$$\Psi_i=\begin{bmatrix} 1 & \rho \\ \rho & 1 \end{bmatrix} \tag{37}$$

Employing the Cholesky decomposition of P_i, A_i can be obtained as a 2 × 2 matrix such that $\Psi_i = A_i A_i^T$. Then, based on A_i, (U_1, U_2) is transformed into (V_1, V_2) by

$$(V_1, V_2) = A_i^{-1}(U_1, U_2) \tag{38}$$

Then, $\Delta D_{sk,i}$ and $S_{l,i}$ are obtained through

$$\Delta D_{sk,i} = F_{D_{sk,i}}^{-1}(V_1), S_{l,i} = F_{S_{l,i}}^{-1}(V_2) \tag{39}$$

The parameters used in the computational process are summarized in **Table 1**. Also, various maintenance schemes are considered: no maintenance, preventive maintenance, and essential maintenance (i.e., replacement only, enhancement only, and both preventive maintenance & replacement).

Time-dependent reliability analysis

Based on the methods presented in the "PDF oriented Reliability Analysis" section, 999 representative points are selected based on Sobol' sequences (Radović *et al.* 1996) for the PDF oriented reliability analysis, whose principal algorithms are in Algorithm 1. All scenarios are coded using MATALB and run on Intel (R) Core (TM) i7-7700 CPU@3.6 GHz and 20 GB of RAM.

Time-dependent reliability without maintenance

Given no maintenance, the PDF of $p_G(g, t)$ (Eq.(16)) and $p^*_G(g, t)$ (Eq.(17)) could be computed through the PDEM and imposing absorbing boundary condition, and that of $p_{G^*}(g^*, t)$ (Eq.(20)) could be calculated by the proposed PKDE and establishing equivalent extreme performance function. The computation times for solving Eq.(16), Eq.(17), Eq.(20), and MCS are 199 s, 193 s, 13 s, and 7406 s, respectively, indicating that PKDE is the most efficent, followed by PDEM,

for the scenarios of no maintenance. **Figs. 5a,b,c,** and **d** show that $p^*_G(g, t)$ is close to $p_G(g, t)$, but the former does not have a negative part. Besides, comparing **Figs.5c** and **d** with **e** and **f**, the surface and contour of $p_{G^*}(g^*, t)$ are rougher than those of $p^*_G(g, t)$. This is due to the fact that the intensity of S_l varies with time, which causes fluctuations in the performance function. Besides, the equivalent extreme performance function could make the performance function monotonic and stable.

Furthermore, $P_f(t)$ is calculated by integrating $p_G(g, t)$, $p^*_G(g, t)$, and $p_{G^*}(g^*, t)$, respectively, which are compared with MCS, as presented in **Fig. 6**. As shown, all $P_f(t)$ and $\beta(t)$ of PDEM and PKDE except for $p_G(g, t)$ are consistent with those from MCS. Although $P_f(t)$ and $\beta(t)$ of $p_G(g, t)$ are initially consistent with other results, they gradually differ significantly from those from $p^*_G(g, t)$, $p_{G^*}(g^*, t)$, and MCS.

For instance, P_f (40) for $p_G(g, t)$ is only 0.060, which is much lower than that of other methods (0.131); and $\beta(40)$ for $p_G(g, t)$ is 1.554, which is higher than that of other methods (1.122). Thus, the failure probability of aging structures might be underestimated if the first-passage problem is not considered. In addition, the $P_f(t)$ and $\beta(t)$ for both $p^*_G(g, t)$ and $p_{G^*}(g^*, t)$ are the same with the results calculated using the MCS, indicating that both the absorption boundary condition and the equivalent limit performance can handle the first-passage problem.

Effect of preventive maintenance on time-dependent reliability

With respect to preventive maintenance, the computational times of PDEM, PKDE, and MCS are 145 s, 22 s, and 6884 s, respectively, which also suggests the efficiency of PKDE is the highest. In addition, results show that $p^*_G(g, t)$ is different from $p_{G^*}(g^*, t)$, as illustrated in **Fig.**

7. By considering maintenance, the PDF of $p^*_G(g, t)$ changes abruptly in the 5th year as indicated in **Figs. 7a** and **b**, while there exists no apparent change between $p_{G^*}(g^*, t)$ in **Figs. 5e** and **f** and **Figs. 7c** and **d**. Despite that preventive maintenance is applied, the PDF surface of $p_{G^*}(g^*, t)$ still looks smooth.

Then, $P_f(t)$ and $\beta(t)$ calculated by $p^*_G(g, t)$ and $p_{G^*}(g^*, t)$ are compared with MCS. As indicated in **Fig. 8**, it can be seen that both $P_f(t)$ and $\beta(t)$ calculated using $p^*_G(g, t)$ and $p_{G^*}(g^*, t)$ agree well with the results from MCS. This shows that the absorption boundary condition and the equivalent limit performance can handle the first-passage problem by considering preventive maintenance. However, in **Fig. 8**, the $P_f(t)$ calculated using $p_{G^*}(g^*, t)$ is closer to MCS than $p^*_G(g, t)$, which shows the accuracy of PKDE may be higher than that of PDEM. In addition, compared to **Fig. 6a**, P_f after 40 years decreases 0.0399 from 0.131 to 0.092, and β after 40 years increases by 0.207 from 1.122 to 1.329.

Essential maintenance on time-dependent reliability

With respect to the effects of replacement on structural performance, the computational times of PDEM, PKDE, and MCS are 199 s, 24 s, and 5213 s, respectively and PKDE is still the most efficient. Besides, the PDF surface and contour of $p^*_G(g, t)$ with those of $p_{G^*}(g^*, t)$ are compared in **Fig. 9**. Due to the involvement of absorbing boundary condition, the second time of maintenance can not be identified by using PDEM as indicated in **Figs. 9a** and **b**. Thus, there is only one time (i.e., at the 15^{th} year) maintenance-induced change as indicated in **Figs. 9a** and **b**, but there are two maintenance-induced changes in the 15th and 29th years in **Figs. 9c** and **d** by using PKDE. Apart from that, the PDF of $p_{G^*}(g^*, t)$ is associated with some cyclical

phenomena.

Also, **Fig. 10** shows the comparison between the $P_f(t)$ and $\beta(t)$ calculated by $p^*_G(g, t)$ and $p_{G*}(g^*, t)$ with MCS. The $P_f(t)$ and $\beta(t)$ of $p_{G*}(g^*, t)$ and MCS show periodically repeat between 0-14 years, 14-29 years, and 29-40 years, but those of $p^*_G(g, t)$ is a monotonic function. Also, the $P_f(t)$ and $\beta(t)$ of $p_{G*}(g^*, t)$ are consistent with MCS. Thus, PDEM with absorbing boundary condition is inappropriate in the scenarios with essential maintenance. Besides, $P_f(t)$ might be underestimated if the absorbing boundary condition is not applied in PDEM, as illustrated in **Fig. 6**. The primary reason is that PDEM relies on the computation of GDEE and relating boundary conditions. However, unlike PDEM, the proposed PKDE requires only the performance functions of representative points without extra conditions. Thus, it proves that PKDE is more practical and flexible in reliability analysis, especially for the scenarios of essential maintenance.

In addition, two types of combined maintenance actions: enhancement and preventive maintenance & replacement are investigated, where for the former scenario, PKDE and MCS cost 10 s and 3634 s, respectively; for the latter one, PKDE and MCS cost 12 s and 1602 s, respectively. Comparing the PDF of enhancement (**Figs. 11a** and **b**) with that of replacement (**Figs.9c** and **d**), the PDF after the 15th year is upwardly increased by 0.2. In addition, comparing preventive maintenance (**Figs. 11c** and **d**) with PDFs of replacement (**Figs. 9c** and **d**), the first maintenance is deferred by two years and the second one is by four years. Thus, it can be indicated that the effect of essential maintenance on PDF surfaces can be obtained by establishing equivalent extreme performance.

Moreover, **Fig. 12** shows that the $P_f(t)$ and $\beta(t)$ calculated by $p_G{}^*(g^*, t)$ with MCS under different scenarios of essential maintenance. Before the 15th year, all the curves are similar, but after the 15^{th} year, the results are different for the two essential maintenance scenarios, where $P_f(t)$ and $\beta(t)$ are monotonic functions for replacement, but periodic between years 16-33 and 33-40 for the other one. Furthermore, the calculations indicate that the proposed PKDE can accurately compute not only the reliability index but also the time instances of maintenance actions.

Conclusions

In this paper, a general framework for time-dependent reliability analysis is established by integrating various deterioration mechanisms, maintenance, and the correlation between load effects and deterioration. Within the framework, a novel PKDE-based reliability analysis method is proposed and validated by numerical cases. The following conclusions are drawn:

(1) According to the numerical analysis, the efficiency and accuracy of the proposed framework are demonstrated by MCS. Both progressive and sudden shocks and their effects on the performance function and reliability are captured by PDF oriented approaches. Also, both the classical PDEM and the proposed PKDE are applied for reliability analysis in the no maintenance cases. However, for PDEM, the structural reliability might be highly overestimated without imposing the absorbing boundary condition.

(2) The PDF surface of PKDE is much smoother than PDEM due to the establishment of an equivalent extreme performance function; also, both the results of reliability analysis

by PKDE and PDEM agree with MCS for the scenarios with preventive maintenance. For the scenarios with essential maintenance, the reliability of PDEM as a function of time is a non-increasing function, unlike MCS and PKDE. Thus, for the cases considering essential maintenance, PKDE is more appropriate than PDEM.

(3) Calculation results demonstrate that compared with replacement, enhancement can effectively reduce the times of maintenance times during the service life. Furthermore, once the preventive maintenance and replacement are performed, the timing of maintenance can be postponed. With PKDE, the critical time instants when maintenances occur can be accurately recognized.

Overall, it is feasible to apply the proposed framework and PKDE to the life-cycle design and maintenance of civil infrastructure by considering different deterioration scenarios and maintenance actions within the service life. In the future, a more advanced and complex deterioration model and complicated load stochastic processes can be implemented in time-dependent reliability analysis to improve the robustness of the proposed framework. Besides, the proposed method might cause oscillations in the PDF tails, which might affect the precision of rare event estimation, and more improvements to the proposed method are needed in the future. In addition, a single-loop strategy will be adopted to integrate with surrogate model-based reliability analysis and reliability-based optimization design.

Appendix:

A. Botev *et al.* ’s Plug-in bandwidth selection method

Botev *et al.* (2010) pointed out that the Gaussian kernel is the unique solution to the diffusion

partial differential equation (Botev *et al.* 2010):

$$\frac{\partial \hat{f}(x,h)}{\partial h} = \frac{1}{2}\frac{\partial^2}{\partial x^2}\hat{f}(x,h), x \in \chi, h > 0 \tag{A-1}$$

where $\chi \equiv R$ and initial condition $\hat{f}(x,0)$ is the sum of a series of δ function. Assuming that f'' is a continuous square-integrable function, the square of the optimal value h of Gaussian kernel density estimator is the minimum of the first-order asymptotic approximation of MISE:

$${}_*h^2 = \left(2N\sqrt{\pi}\left\|f''\right\|^2\right)^{-0.4} \tag{A-2}$$

The main issue is to estimate the $\left\|f''\right\|^2$ in Eq.(A-2). Considering the $\left\|f^j\right\|^2$ for arbitrary integer $j \geq 1$ and denoting unknown $\left\|f^{j+1}\right\|^2$ as $\left\|\widehat{f^{j+1}}\right\|^2$, the square of bandwidth ${}_*\hat{h}_j$ can be evaluated as

$${}_*\hat{h}_j = \left(\frac{1+1/2^{j+1/2}}{3}\frac{1\times 3\times 5\cdots\times(2j-1)}{N\sqrt{\pi/2}\left\|\widehat{f^{j+1}}\right\|^2}\right)^{2/(3+2j)} \tag{A-3}$$

in which $\left\|\widehat{f^{j+1}}\right\|^2$ needs the estimation of ${}_*\hat{h}_{j+1}$. Thus, it proves that estimating ${}_*h$ needs the estimation of a sequence $\left\{{}_*\hat{h}_{j+k}, k \geq 1\right\}$. Denoting the relationship between ${}_*\hat{h}_j$ and ${}_*\hat{h}_{j+1}$ as ${}_*\hat{h}_j = \gamma_j\left({}_*\hat{h}_{j+1}\right)$, the estimation of ${}_*h^2$ can be written as:

$${}_*\hat{h} = \xi\gamma^{[l]}\left({}_*\hat{h}_{j+1}\right), \xi = \left(\frac{6\sqrt{2}-3}{7}\right)^{2/5} \approx 0.90, l > 0 \tag{A-4}$$

where $\gamma^{[k]}(\cdot)$ is the composition, which can be expressed by:

$$\gamma^{[k]}(x) = \gamma_1\left(\gamma_2\left(\cdots\gamma_{k-1}\left(\gamma_k\left(x\right)\right)\right)\right), k \geq 1 \tag{A-5}$$

By employing the fixed-point iteration or the Newtonian method, the estimates of h can be calculated by solving the nonlinear equation Eq.(A-4).

Acknowledgments

Funding: This study has been supported by National Key R&D Program of China (No. 2019YFB1600702), National Natural Science Foundation of China (Grant No. 51808476), and the Research Grants Council of the Hong Kong Special Administrative Region, China (No.: T22-502/18-R and No. PolyU 15219819).

Data Availability

Some or all data, models, or code that support the findings of this study are available from the corresponding author upon reasonable request.

References:

Akiyama, M., Frangopol, D. M., and Ishibashi, H. (2019). "Toward life-cycle reliability-, risk- and resilience-based design and assessment of bridges and bridge networks under independent and interacting hazards: emphasis on earthquake, tsunami and corrosion." *Structure and Infrastructure Engineering*, Taylor & Francis, 0(0), 1–25.

Alibrandi, U., and Mosalam, K. M. (2018). "Kernel density maximum entropy method with generalized moments for evaluating probability distributions, including tails, from a small sample of data." *International Journal for Numerical Methods in Engineering*, 113(13), 1904–1928.

Alibrandi, U., and Ricciardi, G. (2008). "Efficient evaluation of the pdf of a random variable through the kernel density maximum entropy approach." *International Journal for Numerical Methods in Engineering*, 75, 1511–1548.

Andrieu-Renaud, C., Sudret, B., and Lemaire, M. (2004). "The PHI2 method: A way to compute time-variant reliability." *Reliability Engineering and System Safety*, 84(1), 75–86.

Ang, A. H. S., and Tang, W. H. (2007). *Probability Concepts in Engineering Planning: Emphasis on Applications to Civil and Environmental Engineering*. John Wiley and Sons.

Au, S. K., and Beck, J. L. (2003). "Importance sampling in high dimensions." *Structural Safety*, 25(2), 139–163.

Barone, G., and Frangopol, D. M. (2014). "Reliability, risk and lifetime distributions as performance indicators for life-cycle maintenance of deteriorating structures." *Reliability Engineering and System Safety*, Elsevier, 123, 21–37.

Bastidas-Arteaga, E. (2018). "Reliability of Reinforced Concrete Structures Subjected to Corrosion-Fatigue and Climate Change." *International Journal of Concrete Structures and Materials*, Springer Netherlands, 12(1).

669 Botev, Z. I., Grotowski, J. F., and Kroese, D. P. (2010). “Kernel density estimation via
670 diffusion.” *Annals of Statistics*, 38(5), 2916–2957.
671 Chen, J. B., Ghanem, R., and Li, J. (2009). “Partition of the probability-assigned space in
672 probability density evolution analysis of nonlinear stochastic structures.” *Probabilistic*
673 *Engineering Mechanics*, Elsevier Ltd, 24(1), 27–42.
674 Chen, J. B., and Zhang, S. H. (2013). “Improving point selection in cubature by a new
675 discrepancy.” *SIAM Journal on Scientific Computing*, 35(5), A2121–A2149.
676 Chen, J., Yang, J., and Li, J. (2016). “A GF-discrepancy for point selection in stochastic
677 seismic response analysis of structures with uncertain parameters.” *Structural Safety*,
678 Elsevier Ltd, 59, 20–31.
679 Colbrook, M. J., Botev, Z. I., Kuritz, K., and MacNamara, S. (2020). “Kernel density
680 estimation with linked boundary conditions.” *Studies in Applied Mathematics*, (March),
681 1–40.
682 Courant, R., Friedrichs, K., and Lewy, H. (1928). “About the partial difference equations in
683 mathematical physics (Über die partiellen Differenzengleichungen der mathematischen
684 Physik).” *Mathematische Annalen*, 100(1), 32–74.
685 Denton, S. (2002). “Data estimates for different maintenance options for reinforced concrete
686 cross-heads.” *Personal communication for Highways Agency, UK). Parsons*
687 *Brinckerhoff Ltd., Bristol, UK*.
688 Ditlevsen, O., and Madsen, H. O. (1996). *Structural reliability methods*. Wiley New York,
689 New York.
690 Dong, Y., Akiyama, M., Frangopol, D. M., and Tsompanakis, Y. (2020). “Risk-, resilience-,
691 and sustainability-informed assessment and management of civil infrastructure in a life-
692 cycle context.” *Structure and Infrastructure Engineering*, Taylor & Francis, 17(4), 441–
693 442.
694 Enright, M. P., and Frangopol, D. M. (1999). “Maintenance planning for deteriorating
695 concrete bridges.” *Journal of Structural Engineering*, 125(12), 1407–1414.
696 Frangopol, D. M., Dong, Y., and Sabatino, S. (2017). “Bridge life-cycle performance and
697 cost: analysis, prediction, optimisation and decision-making.” *Structure and*
698 *Infrastructure Engineering*, Taylor & Francis, 13(10), 1239–1257.
699 Frangopol, D. M., Kallen, M.-J., and Noortwijk, J. M. van. (2004). “Probabilistic models for
700 life-cycle performance of deteriorating structures: review and future directions.”
701 *Progress in Structural Engineering and Materials*, 6(4), 197–212.
702 Frangopol, D. M., Lin, K.-Y., and Estes, A. C. (1997). “Reliability of reinforced concrete
703 girders under corrosion attack.” *Journal of Structural Engineering*, 123(3), 286–297.
704 Gu, X. L., Guo, H. Y., Zhou, B. Bin, Zhang, W. P., and Jiang, C. (2018). “Corrosion non-
705 uniformity of steel bars and reliability of corroded RC beams.” *Engineering Structures*,
706 Elsevier Ltd, 167(May), 188–202.
707 Guo, H., Dong, Y., Bastidas-arteaga, E., and Gu, X. (2021). “Probabilistic failure analysis ,
708 performance assessment , and sensitivity analysis of corroded reinforced concrete
709 structures Local sensitivity analysis Probabilistic modeling Surrogate modeling
710 Probabilistic analysis.” *Engineering Failure Analysis*, Elsevier Ltd, 124(March), 105328.
711 Guo, H. Y., Dong, Y., and Gu, X. L. (2020a). “Durability assessment of reinforced concrete

712 structures considering global warming: A performance-based engineering and
713 experimental approach." *Construction and Building Materials*, 233, 117251.
714 Guo, H. Y., Dong, Y., and Gu, X. L. (2020b). "Two-step translation method for time-
715 dependent reliability of structures subject to both continuous deterioration and sudden
716 events." *Engineering Structures*, Elsevier Ltd, 225, 111291.
717 El Hassan, J., Bressolette, P., Chateauneuf, A., and El Tawil, K. (2010). "Reliability-based
718 assessment of the effect of climatic conditions on the corrosion of RC structures subject
719 to chloride ingress." *Engineering Structures*, Elsevier Ltd, 32(10), 3279–3287.
720 Hu, Z., and Du, X. (2013). "Time-dependent reliability analysis with joint upcrossing rates."
721 *Structural and Multidisciplinary Optimization*, 48(5), 893–907.
722 Jia, G. F., and Gardoni, P. (2018a). "Simulation-based approach for estimation of stochastic
723 performances of deteriorating engineering systems." *Probabilistic Engineering*
724 *Mechanics*, Elsevier Ltd, 52(June 2017), 28–39.
725 Jia, G. F., Taflanidis, A. A., and Beck, J. L. (2017a). "A new adaptive rejection sampling
726 method using kernel density approximations and its application to subset simulation."
727 *ASCE-ASME Journal of Risk and Uncertainty in Engineering Systems, Part A: Civil*
728 *Engineering*, 3(2), 1–12.
729 Jia, G., and Gardoni, P. (2018b). "State-dependent stochastic models: A general stochastic
730 framework for modeling deteriorating engineering systems considering multiple
731 deterioration processes and their interactions." *Structural Safety*, Elsevier Ltd, 72, 99–
732 110.
733 Jia, G., and Gardoni, P. (2019a). "Stochastic life-cycle analysis and performance optimization
734 of deteriorating engineering systems using state-dependent deterioration stochastic
735 models." *Routledge Handbook of Sustainable and Resilient Infrastructure*, Routledge,
736 580–602.
737 Jia, G., and Gardoni, P. (2019b). "Stochastic life-cycle analysis: renewal-theory life-cycle
738 analysis with state-dependent deterioration stochastic models." *Structure and*
739 *Infrastructure Engineering*, Taylor & Francis, 15(8), 1001–1014.
740 Jia, G., Tabandeh, A., and Gardoni, P. (2017b). "Life-cycle analysis of engineering systems:
741 Modeling deterioration, instantaneous reliability, and resilience." *Risk and Reliability*
742 *Analysis: Theory and Application*, P. Gardoni, ed., Springer, 465–494.
743 Joanni, A., and Rackwitz, R. (2008). "Cost-benefit optimization for maintained structures by a
744 renewal model." *Reliability Engineering and System Safety*, 93(3), 489–499.
745 Kong, J. S., and Frangopol, D. M. (2003). "Life-cycle reliability-based maintenance cost
746 optimization of deteriorating structures with emphasis on bridges." *Journal of Structural*
747 *Engineering*, 129(6), 818–828.
748 Kumar, R., Cline, D. B. H., and Gardoni, P. (2015). "A stochastic framework to model
749 deterioration in engineering systems." *Structural Safety*, Elsevier Ltd, 53, 36–43.
750 Kumar, R., and Gardoni, P. (2014). "Renewal theory-based life-cycle analysis of deteriorating
751 engineering systems." *Structural Safety*, Elsevier Ltd, 50, 94–102.
752 Kumar, R., Gardoni, P., Sanchez-Silva, M., Kumar, R., Gardoni, P., Sanchez-Silva, M.,
753 Kumar1, R., Gardoni, P., and Sanchez-Silva, M. (2009). "Effect of cumulative seismic
754 damage and corrosion on the life-cycle cost of reinforced concrete bridges." *Life-Cycle*

Civil Engineering - Proceedings of the 1st International Symposium on Life-Cycle Civil Engineering, IALCCE '08, Wiley Online Library, 38(7), 887–905.
Li, C. Q., and Melchers, R. E. (2005). "Time-dependent reliability analysis of corrosion-induced concrete cracking." *ACI Structural Journal*, 102(4), 543–549.
Li, J., and Chen, J. B. (2007). "The number theoretical method in response analysis of nonlinear stochastic structures." *Computational Mechanics*, 39(6), 693–708.
Li, J., and Chen, J. B. (2008). "The principle of preservation of probability and the generalized density evolution equation." *Structural Safety*, 30(1), 65–77.
Li, J., and Chen, J. B. (2009). *Stochastic dynamics of structures*. *Physical Review E - Statistical, Nonlinear, and Soft Matter Physics*, John Wiley & Sons.
Li, J., and Chen, J. B. (2014). "Probability density evolution method in stochastic dynamics." *Encyclopedia of Earthquake Engineering*, 1–14.
Li, J., Chen, J. B., Sun, W., and Peng, Y. (2012). "Advances of the probability density evolution method for nonlinear stochastic systems." *Probabilistic Engineering Mechanics*, Elsevier Ltd, 28, 132–142.
Liu, B., Zhao, X., Liu, G., and Liu, Y. (2020). "Life cycle cost analysis considering multiple dependent degradation processes and environmental influence." *Reliability Engineering and System Safety*, Elsevier Ltd, 197(March 2019), 106784.
Lu, Z. H., Cai, C. H., Zhao, Y. G., Leng, Y., and Dong, Y. (2020). "Normalization of correlated random variables in structural reliability analysis using fourth-moment transformation." *Structural Safety*, Elsevier, 82(August 2019), 101888.
Lutes, L. D., and Sarkani, S. (2004). *Random Vibrations: Analysis of Structural and Mechanical Systems*. *Random Vibrations: Analysis of Structural and Mechanical Systems*, Butterworth-Heinemann.
Mori, Y., and Ellingwood, B. R. (1993). "Reliability-based service-life assessment of aging concrete structures." *Journal of Structural Engineering*, 119(5), 1600–1621.
Radović, I., Sobol, I. M., and Tichy, R. F. (1996). "Quasi-Monte Carlo methods for numerical integration: Comparison of different low discrepancy sequences." *Monte Carlo Methods and Applications*, 2(1), 1–14.
Rawa, M. J. H., Thomas, D. W. P., and Sumner, M. (2011). "Simulation of non-linear loads for harmonic studies." *Proceeding of the International Conference on Electrical Power Quality and Utilisation, EPQU*, 00037, 102–107.
Sanchez-Silva, M., Klutke, G. A., and Rosowsky, D. V. (2011). "Life-cycle performance of structures subject to multiple deterioration mechanisms." *Structural Safety*, Elsevier Ltd, 33(3), 206–217.
Saydam, D., Frangopol, D. M., and Dong, Y. (2013). "Assessment of risk using bridge element condition ratings." *Journal of Infrastructure Systems*, 19(3), 252–265.
Sheather, S. J., and Jones, M. c. (1991). "A Reliable Data-Based Bandwidth Selection Method for Kernel Density Estimation." *Journal of the Royal Statistical Society. Series B*, 53(3), 683–690.
Silverman, B. W. (1986). *Density estimation for statistics and data analysis*. CRC press.
Stewart, M. G., and Al-Harthy, A. (2008). "Pitting corrosion and structural reliability of corroding RC structures: Experimental data and probabilistic analysis." *Reliability*

Engineering and System Safety, 93(3), 373–382.
Sudret, B. (2008). “Analytical derivation of the outcrossing rate in time-variant reliability problems.” *Structure and Infrastructure Engineering*, 4(5), 353–362.
Thompson, P. D., Small, E. P., Johnson, M., and Marshall, A. R. (1998). “The Pontis Bridge Management System.” *Structural Engineering International: Journal of the International Association for Bridge and Structural Engineering (IABSE)*, 8(4), 303–308.
Tran, T. V., Bastidas-Arteaga, E., Schoefs, F., Bonnet, S., O’Connor, A. J., and Lanata, F. (2012). “Structural reliability analysis of deteriorating RC bridges considering spatial variability.” *Bridge Maintenance, Safety, Management, Resilience and Sustainability - Proceedings of the Sixth International Conference on Bridge Maintenance, Safety and Management*, (October 2015), 698–705.
Tu, B., Fang, Z., Dong, Y., and Frangopol, D. M. (2017). “Time-variant reliability analysis of widened deteriorating prestressed concrete bridges considering shrinkage and creep.” *Engineering Structures*, Elsevier Ltd, 153, 1–16.
Wang, C., Li, Q., and Ellingwood, B. R. (2016). “Time-dependent reliability of ageing structures: an approximate approach.” *Structure and Infrastructure Engineering*, Taylor & Francis, 12(12), 1566–1572.
Wang, C., and Zhang, H. (2018). “Roles of load temporal correlation and deterioration-load dependency in structural time-dependent reliability.” *Computers and Structures*, Elsevier Ltd, 194, 48–59.
Wang, C., Zhang, H., and Li, Q. (2017). “Reliability assessment of aging structures subjected to gradual and shock deteriorations.” *Reliability Engineering and System Safety*, Elsevier, 161(January), 78–86.
Wang, Z. J., Dong, Y., and Jin, W. L. (2020). “Life-cycle cost analysis of deteriorating civil infrastructures incorporating social sustainability.” *Journal of Infrastructure Systems*, (Accepted).
Wang, Z., Jin, W., Dong, Y., and Frangopol, D. M. (2018). “Hierarchical life-cycle design of reinforced concrete structures incorporating durability, economic efficiency and green objectives.” *Engineering Structures*, Elsevier, 157(November 2017), 119–131.
Zhang, M., Song, H., Lim, S., Akiyama, M., and Frangopol, D. M. (2019). “Reliability estimation of corroded RC structures based on spatial variability using experimental evidence, probabilistic analysis and finite element method.” *Engineering Structures*, Elsevier, 192(April), 30–52.
Zhao, J. Z., Fonseca-Sarmiento, C., and Tan, J. (2019). *America’s Trillion-Dollar Repair Bill*.

Figure Captions

Fig. 1. Framework for modeling the performance function in a life-cycle context

Fig. 2. Time-dependent performance indicator (e.g., reliability index) by considering deterioration and maintenance

Fig. 3. Schematic diagram of equivalent extreme and original performance functions

Fig. 4. Comparison of PDF estimation by using different methods

Fig. 5. Comparisons of PDF surface and contour in the scenario of no maintenance: PDF surface of (a) $p_G(g, t)$, (b) $p_G(g, t)$, (c) $p^*_G(g, t)$, (d) $p^*_G(g, t)$, (e) $p_{G^*}(g^*, t)$, and (f) $p_{G^*}(g^*, t)$

Fig. 6. Comparison of MCS, PDEM, and PKDE: (a)$P_f(t)$ and (b) $\beta(t)$

Fig. 7. Comparisons of PDF surface and contour in the scenario by considering preventive maintenance: PDF surface by (a) $p^*_G(g, t)$, (b) $p^*_G(g, t)$, (c) $p_{G^*}(g^*, t)$, and (d) $p_{G^*}(g^*, t)$

Fig. 8. Comparison of MCS, PDEM, and PKDE in the scenario by considering preventive maintenance: (a) $P_f(t)$ and (b) $\beta(t)$

Fig. 9. Comparisons of PDF surface and contour in the scenario by considering replacement: (a) $p^*_G(g, t)$, (b) $p^*_G(g, t)$, (c) $p_{G^*}(g^*, t)$, and (d) $p_{G^*}(g^*, t)$

Fig. 10. Comparison of MCS, PDEM, and PKDE in the scenario by considering preventive maintenance: (a) $P_f(t)$ and (b) $\beta(t)$

Fig. 11. Comparisons of PDF surface and contour of $p_{G^*}(g^*, t)$ in the different scenarios: (a) PDF surface of enhancement, (b) PDF contour of enhancement, (c) PDF surface of preventive maintenance & replacement, and (d) PDF contour of preventive maintenance & replacement

Fig. 12. Comparison of MCS, PDEM, and PKDE in the scenarios by considering enhancement

and preventive maintenance & replacement: (a) $P_f(t)$ and (b) $\beta(t)$

Table

Table 1 Parameters used in the example

Parameters	Values	Parameters	Values	Parameters	Values	Parameters	Values
μ_{R0}	1.0	δ_{R0}	0.05	a	2×10^{-6}	b	3
μ_d	0.1	δ_d	0.3	β_{c1}	2.5	β_{c2}	2.0
μ_l	0.1	δ_l	0.3	λ	0.1/year	R_{en}	0.2
μ_{sk}	0.02	δ_{sk}	0.3	ρ	0.5		

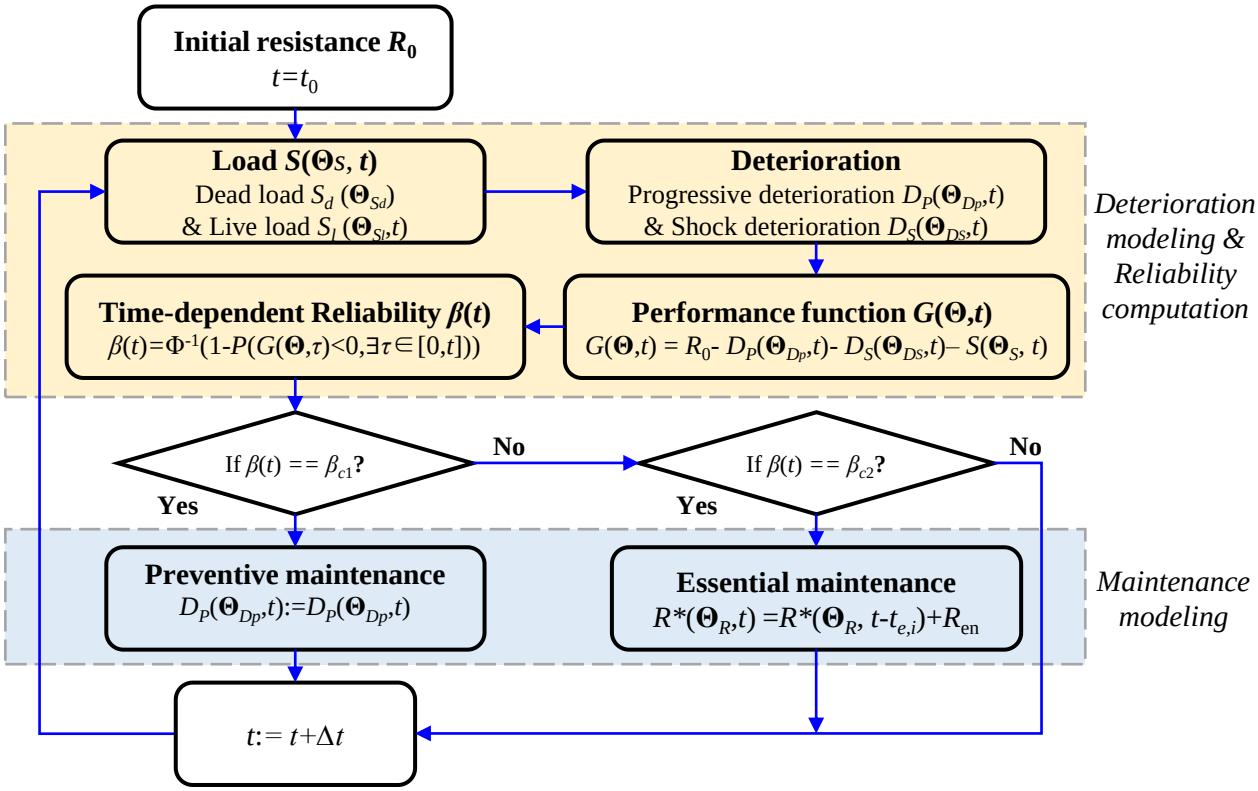

Fig.1

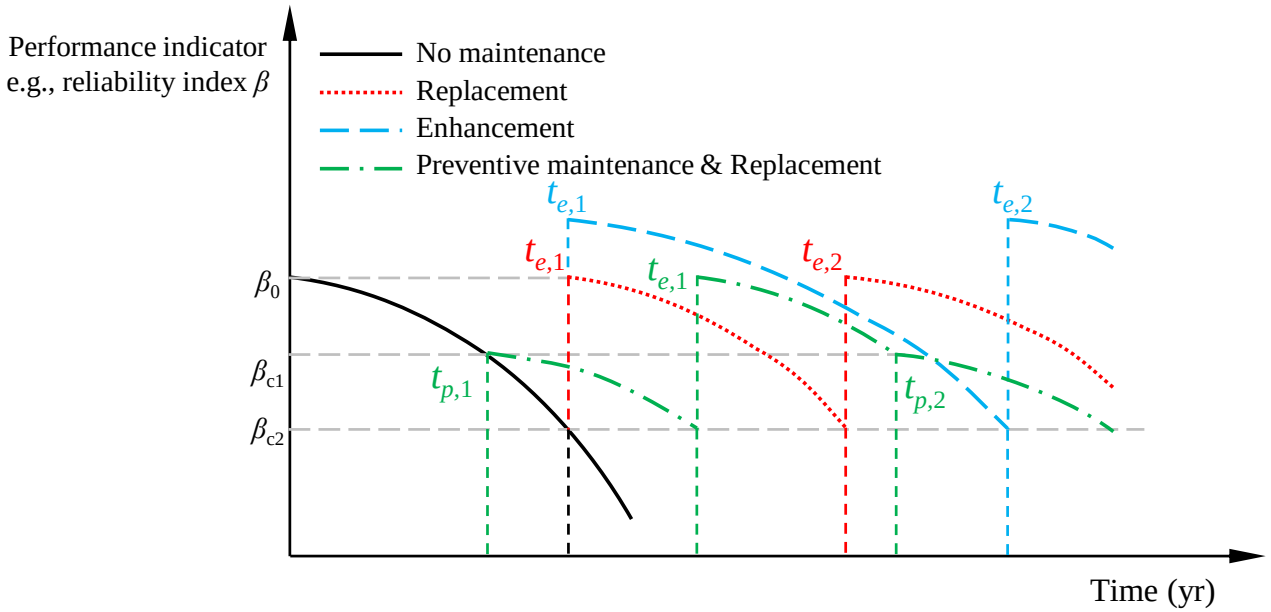
Performance indicator
e.g., reliability index β
No maintenance
Replacement
Enhancement
Preventive maintenance & Replacement
$t_{e,1}$
$t_{e,2}$
$t_{e,1}$
$t_{e,1}$
$t_{e,2}$
β_0
β_{c1}
β_{c2}
$t_{p,1}$
$t_{p,2}$
Time (yr)

Fig.2

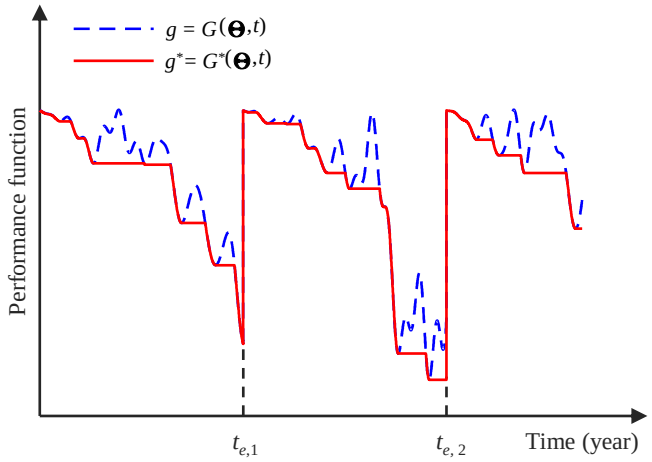
$g = G(\boldsymbol{\Theta},t)$
$g^* = G^*(\boldsymbol{\Theta},t)$
Performance function
$t_{e,1}$
$t_{e,2}$
Time (year)

Fig.3

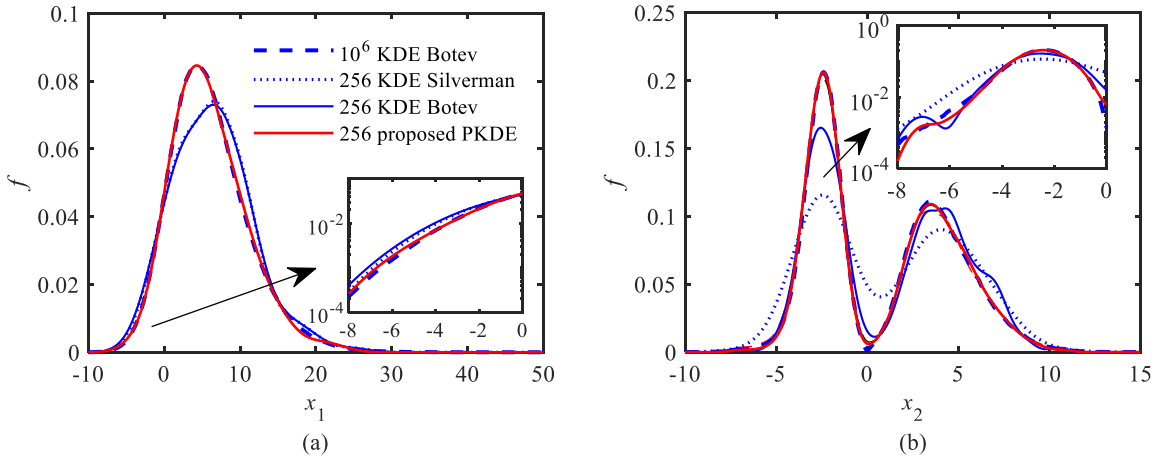
0.1
0.08
0.06
0.04
0.02
0
f
-10
0
10
20
30
40
50
x_1
10^6 KDE Botev
256 KDE Silverman
256 KDE Botev
256 proposed PKDE
10^{-2}
10^{-4}
-8
-6
-4
-2
0
(a)
0.25
0.2
0.15
0.1
0.05
0
f
-10
-5
0
5
10
15
x_2
10^0
10^{-2}
10^{-4}
-8
-6
-4
-2
0
(b)

Fig.4

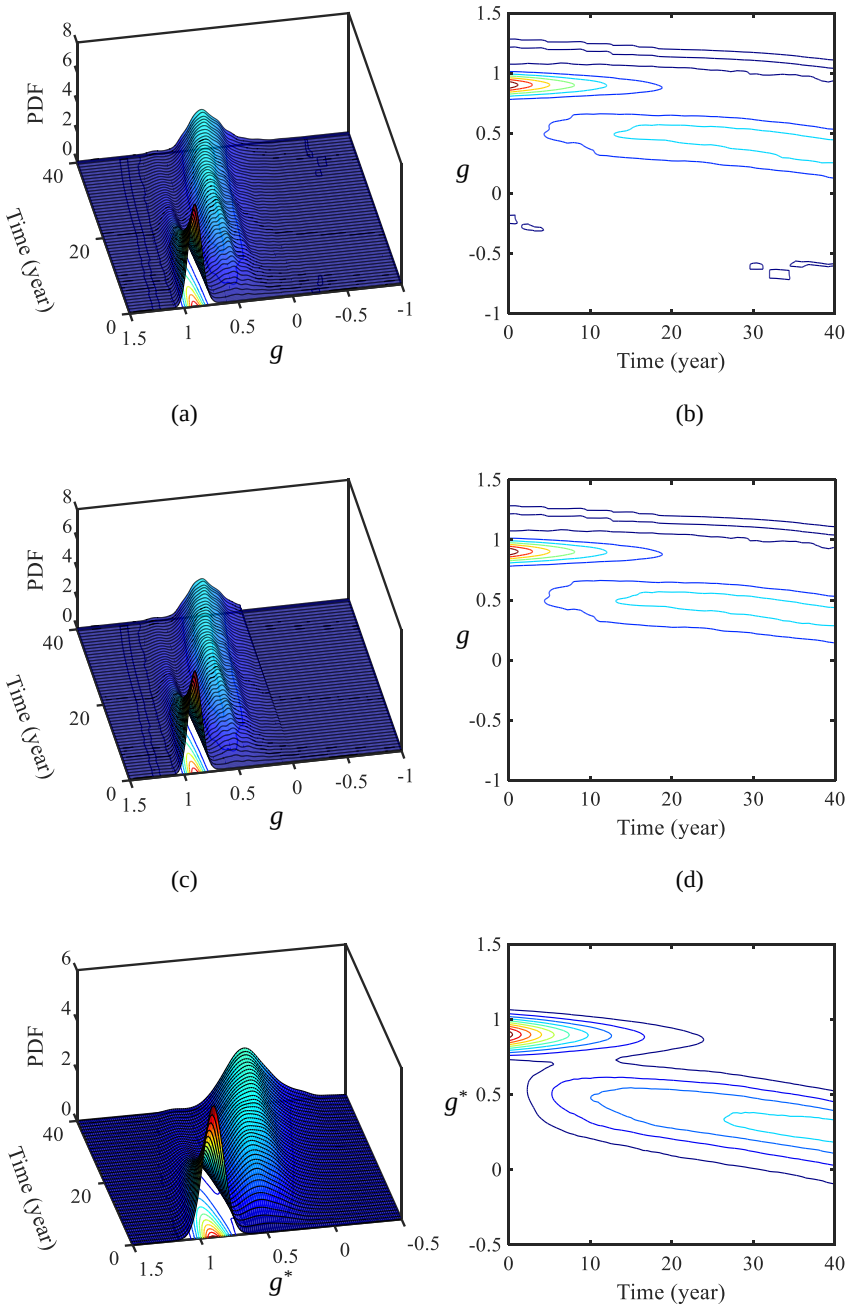

Fig.5

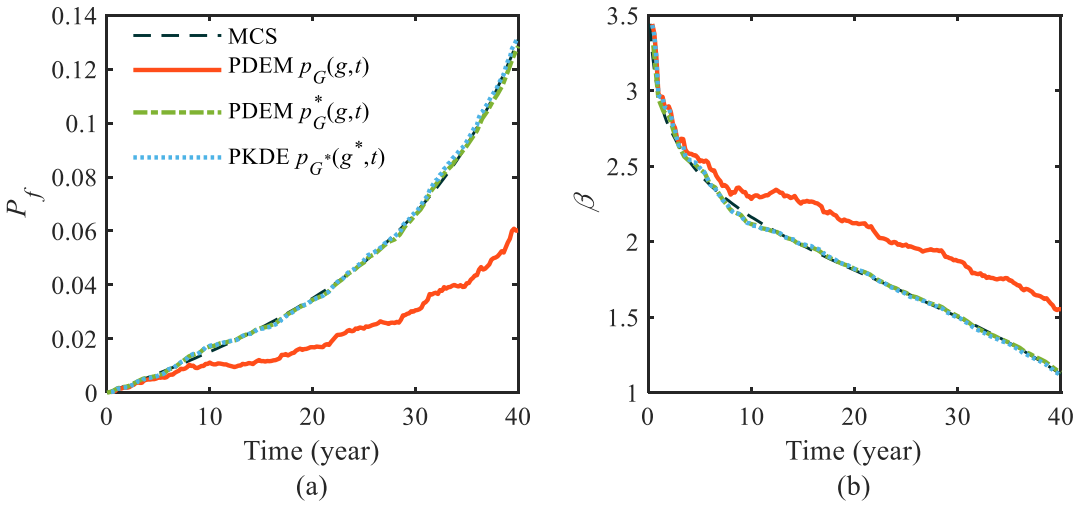
MCS
PDEM $p_G(g,t)$
PDEM $p^*_G(g,t)$
PKDE $p_{G^*}(g^*,t)$
P_f
β
Time (year)
Time (year)
(a)
(b)

Fig.6

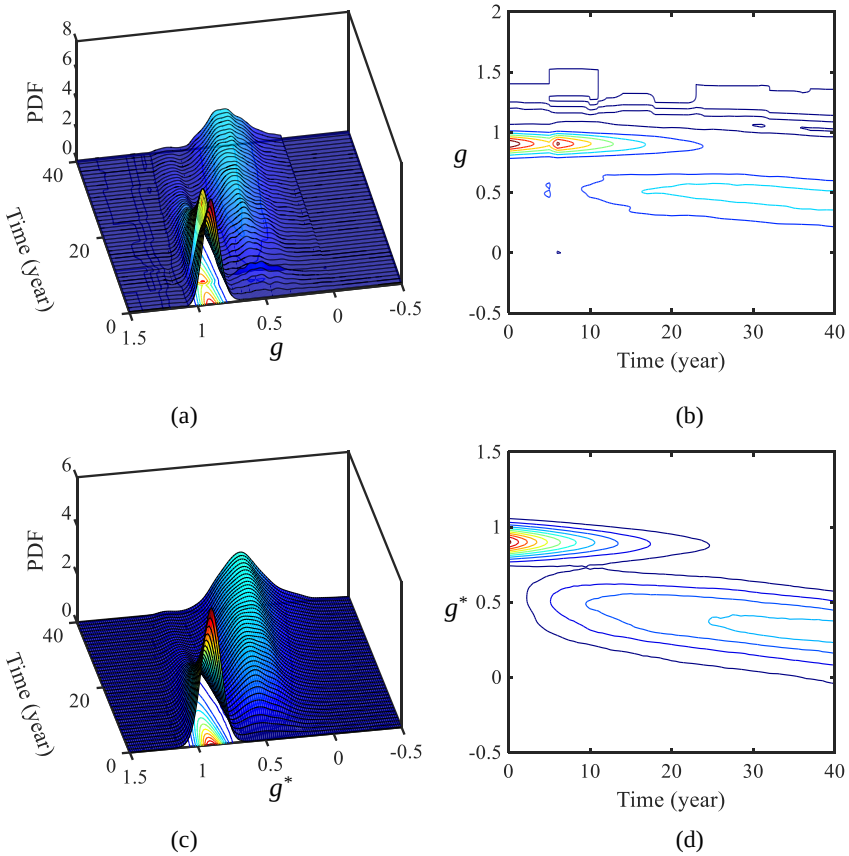

Fig.7

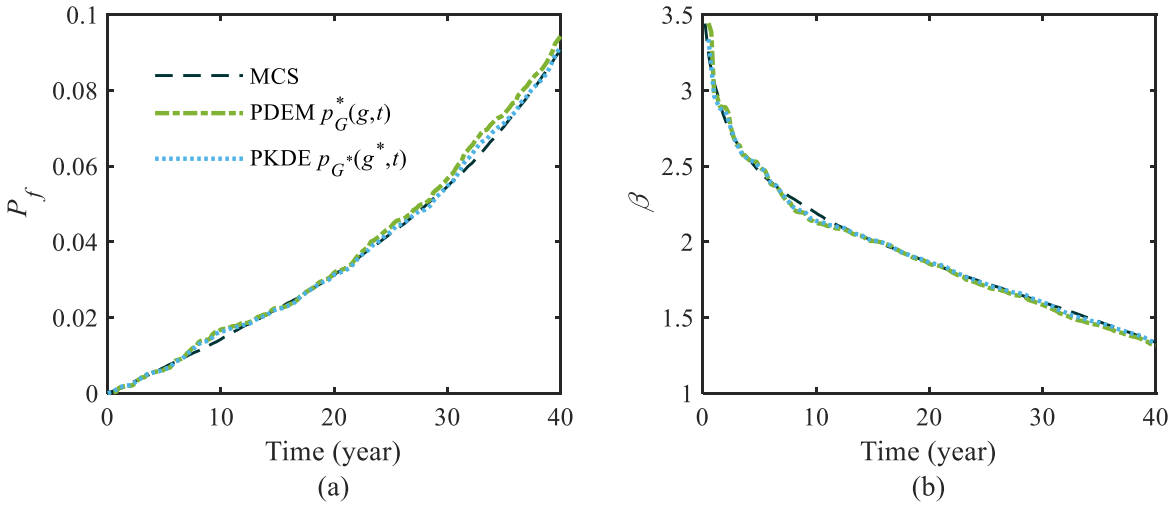
0.1
0.08
0.06
0.04
0.02
0
P_f
MCS
PDEM $p^*_G(g,t)$
PKDE $p_{G^*}(g^*,t)$
0
10
20
30
40
Time (year)
(a)
3.5
3
2.5
2
1.5
1
β
0
10
20
30
40
Time (year)
(b)

Fig.8

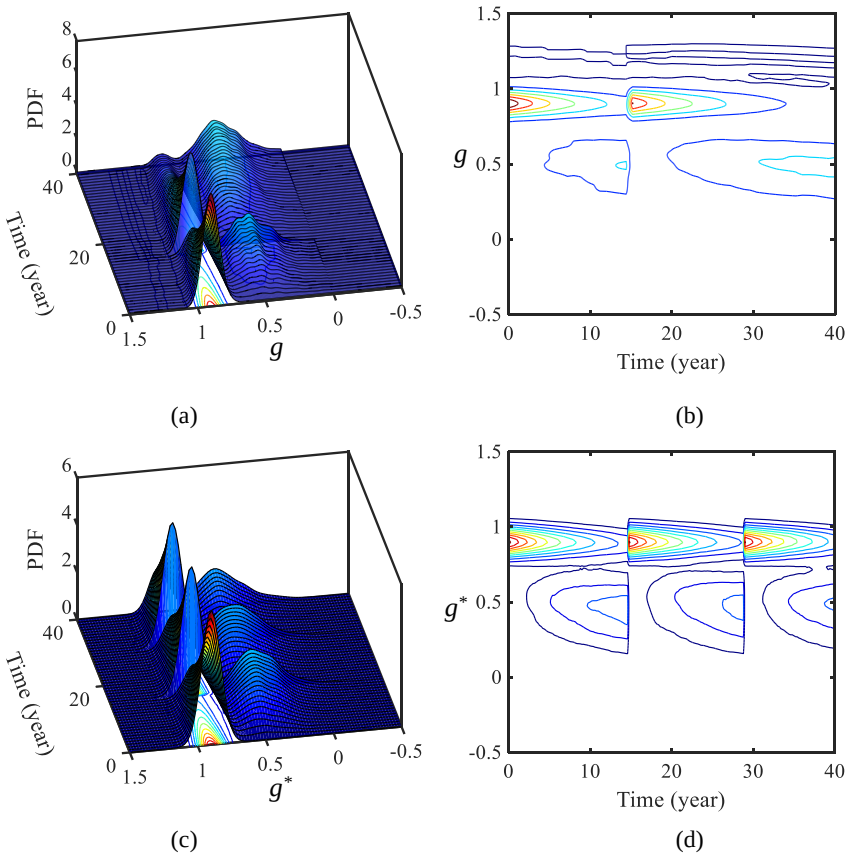

Fig.9

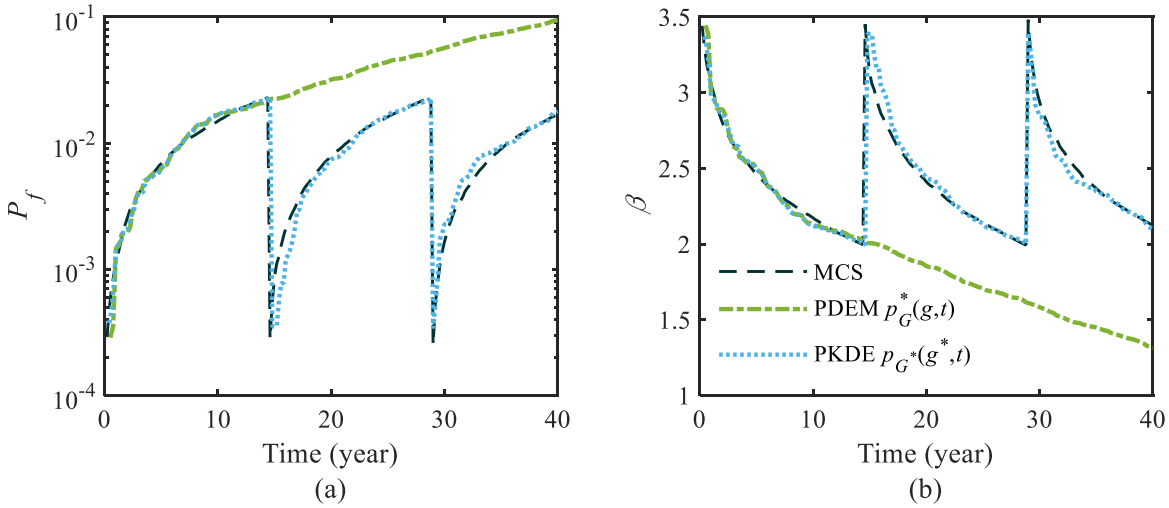
10^{-1}
10^{-2}
10^{-3}
10^{-4}
P_f
0
10
20
30
40
Time (year)
(a)
3.5
3
2.5
2
1.5
1
β
MCS
PDEM $p^*_G(g,t)$
PKDE $p_{G^*}(g^*,t)$
0
10
20
30
40
Time (year)
(b)

Fig.10

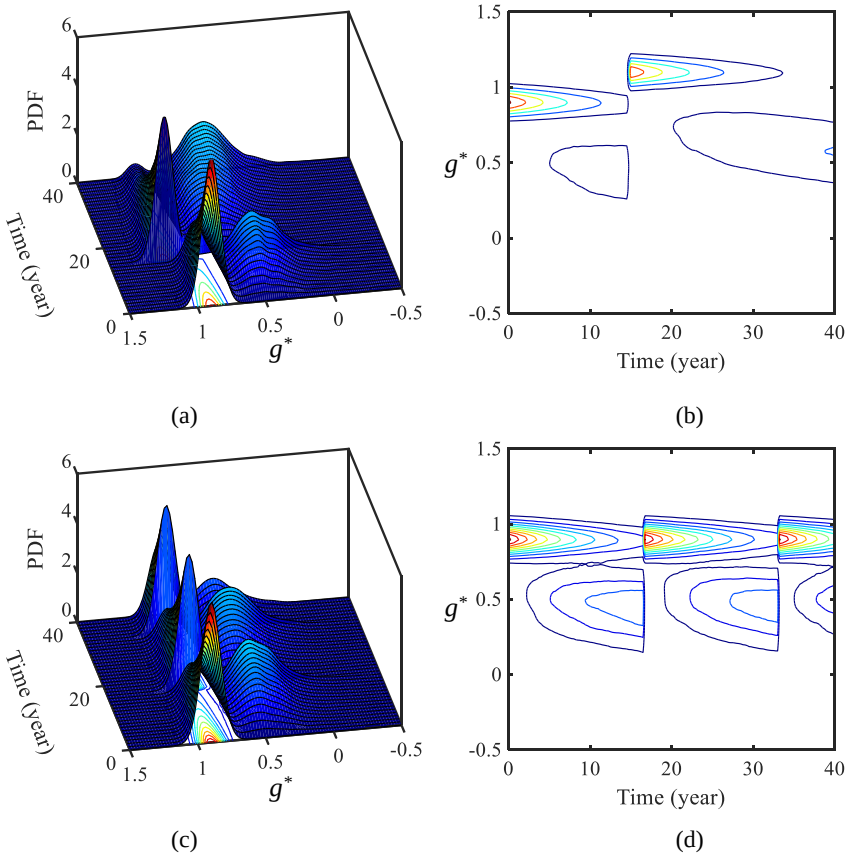

Fig.11

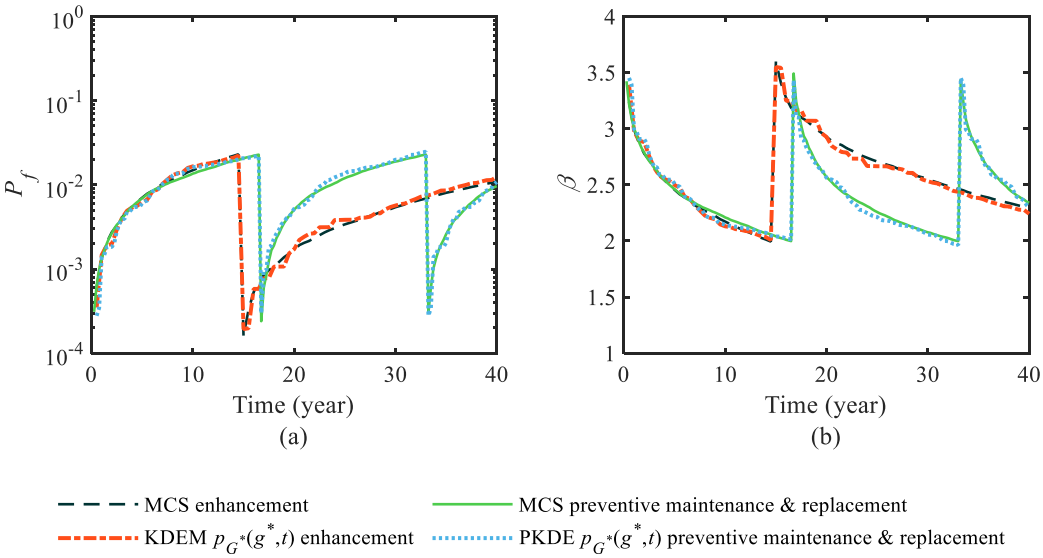
10^0
10^{-1}
10^{-2}
10^{-3}
10^{-4}
P_f
0
10
20
30
40
Time (year)
(a)
4
3.5
3
2.5
2
1.5
1
β
0
10
20
30
40
Time (year)
(b)
MCS enhancement
MCS preventive maintenance & replacement
KDEM $p_{G^*}(g^*,t)$ enhancement
PKDE $p_{G^*}(g^*,t)$ preventive maintenance & replacement

Fig.12